Control Structures for Low-Emission Combustion in Multi-Cylinder Engines

Henningsson, Maria

2008

Document Version:
Publisher's PDF, also known as Version of record

Control Structures for Low-Emission Combustion in Multi-Cylinder Engines

Maria Karlsson

Department of Automatic Control
Lund University
Lund, March 2008

To Toivo

Department of Automatic Control
Lund University
Box 118
SE-221 00 LUND
Sweden

ISSN 0280–5316
ISRN LUTFD2/TFRT--3243--SE

Printed in Sweden,
Lund University, Lund 2008

Abstract

Traditionally, heavy-duty diesel engines have high efficiencies but also high emissions of NO_x and soot particles. New engine concepts show the potential to retain diesel-like efficiencies while reducing emissions by forming a completely or partially homogeneous mixture of fuel and air prior to ignition through compression. The long ignition delay required to form this homogeneous mixture makes the combustion process less predictable and inherently more difficult to control.

This thesis summarizes work on control structures for three different set-ups of such low-emissions combustion engines. In a port-fuel injection engine, it was shown that combining two control variables in a mid-ranging control structure can address the problem of actuator saturation. In a fumigation engine, control was proven to be a powerful tool for automatic calibration in a laboratory setting. In a direct-injection engine, LQG controllers were designed to optimize an emissions trade-off cost function during transients. Experiments were performed on a six-cylinder heavy-duty engine, and multi-cylinder effects and complications were explicitly considered in the work.

Acknowledgements

When I first heard of the combustion engine control project during my first weeks as a Ph.D. student, I knew practically nothing about engines and had some trouble imagining myself working in this field. However, after some encouragement from my to-be supervisor, Rolf Johansson, the project seemed more and more appealing in the possibility of combining theory with practical experiments. It has been very rewarding to work on the project, and to learn more about the very current field of combustion engines.

During this time, I have had great support from my main supervisor, Rolf, who has a profound knowledge of most any topic that comes up to discussion. Most of the work presented here was performed in close collaboration with fellow Ph.D. student Kent Ekholm at the department of Energy Sciences. I believe Kent is the perfect complement to myself in his very practical competence and approach, and I hope we can continue to strengthen and complement each other. I have had two co-supervisors: Per Tunestål whose feedback and suggestions are always helpful and well thought through, and Per Hagander who started as the very enthusiastic supervisor of my master's thesis, and has continued to provide enthusiastic feedback during my Ph.D. studies.

Throughout the project, we have had great support from Stefan Strömberg, Petter Strandh, and Johan Bengtsson at Volvo Powertrain. I am very grateful for the great work Petter and Johan put into the predecessor of this project, and especially for implementing `dapmeas`, our exceptional control system. Petter has always been very helpful with all practical issues throughout the project. Financial support from Vinnova under the grant PFF 2005-00180, *Diesel-HCCI in Multi-Cylinder Engines*, is gratefully acknowledged.

I have enjoyed performing the experimental work in the combustion engine lab at the department of Energy Sciences. The engine lab has good facilities and a team of skilled technicians to help keep the engines running. In the process of planning the next step in the research project, Bengt Johansson has been an endless source of ideas.

The department of Automatic Control provides a very beneficial environment for Ph.D. studies, that I am glad to be a part of. Everyone at the department contributes to this great environment, but I would especially like to mention Anders Widd for proof-reading this thesis

and sharing the interest in combustion engine control, Leif Andersson and Anders Blomdell for providing outstanding computer support, and Britt-Marie Mårtensson, Eva Schildt, and Agneta Tuszynski for keeping the department together. I would also like to thank all those who eat their lunch in the lunch room and who are very willing to share their parenting and grandparenting experiences.

Finally, I am so very lucky to have Toivo by my side. You have an enormous patience and you are a constant source of support, inspiration, and love. I very much look forward to the exciting times ahead of us ...

Contents

1

Introduction

1.1 Context

As automotive traffic rapidly increases world-wide, the negative environmental and human health effects become more and more clear. The main components of combustion engine emissions are carbon dioxide CO_2, water, unburned hydrocarbons HC, carbon monoxide CO, oxides of nitrogen NO_x, and soot particles PM. In the era of global warming concern, CO_2 emissions attract much medial attention. To minimize CO_2 emissions for a combustion engine running on any given fuel, the engine efficiency should be maximized.

Compression ignition (CI) engines dominate the market for heavy-duty commercial vehicles because their over-all efficiency is superior to that of the other main engine type, the spark ignition (SI) engine. The disadvantage of the CI engine is mainly high levels of emissions of NO_x and PM. NO_x and PM emissions are linked to a broad range of environmental and human health effects including eutrophication of water bodies, acid rain, smog, and increased frequency of diseases such as asthma and lung cancer [Environmental Protection Agency, 2001].

As a response to the findings of the effects of NO_x and PM emissions, legislators have imposed increasingly stringent emissions standards over the past 10–15 years. Figure 1.1 shows legislated emissions levels for Europe and the U.S. from 1990 to 2010 [DieselNet,

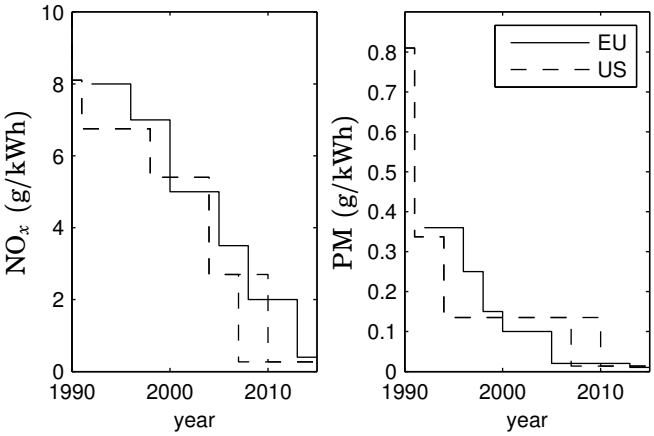

Figure 1.1 Legislated emission levels for heavy-duty vehicles in the European Union and United States. New U.S. standards were introduced on a 50 % of sales basis in 2007 and will take full effect in 2010. EU standards from 2013 are not yet finalized.

2008; DieselNet, 2007]. Emissions legislation has provided the incentive to develop and introduce new technology to reduce emissions from heavy-duty vehicles, and still continues to do so. Especially noteworthy in Figure 1.1 are the dramatically tightened U.S. requirements that will take full effect in 2010, with similar levels being proposed in the European Union from 2013.

To comply with such stringent legislation, a shift in technology is necessary. The currently dominating method of meeting the requirements is to introduce an exhaust aftertreatment system where PM is removed in a diesel particulate filter, and NO_x is removed using selective catalytic reduction (SCR) which allows for reduction of NO_x in the oxygen-excess exhausts by the aid of a reductant, typically urea.

An alternative to such advanced and costly aftertreatment systems is to modify the combustion process such that engine-out emissions are sufficiently low to comply with legislation, thus eliminating or reducing the need for aftertreatment. The dominant factor determining NO_x emissions is combustion temperature. If the peak combustion

temperature is kept below approximately 1800 K, virtually no NO_x is formed, but formation increases exponentially with temperatures above the threshold. The diesel combustion process is highly inhomogeneous with diffusion combustion in a flame around the fuel spray. Temperature distribution throughout the flame is non-uniform, with some very hot zones where NO_x is formed.

To reduce formation of NO_x, the peak temperature in the cylinder should be reduced which could be achieved by replacing the diffusion combustion in the fuel spray by combustion of a homogeneous mixture of fuel and air. Unlike in an SI engine, the homogeneous mixture should be ignited by compression alone in order to have a spatially homogeneous combustion process without a flame front. This engine concept is called homogeneous charge compression ignition (HCCI), and holds the promise of combining low emissions of NO_x with high efficiency.

A challenge in making the HCCI engine feasible is control of combustion. Unlike the traditional CI engine where combustion is directly controlled by fuel injection, or the SI engine where combustion is controller by the spark, there is no direct combustion trigger in the HCCI engine. Cycle-to-cycle and cylinder-to-cylinder variations are substantially increased compared to the CI engine, and combustion becomes very sensitive to operating conditions such as speed, load, and engine temperature. The engine must be operated such that combustion timing is kept within a narrow specified range, and that the requirements on emissions and efficiency are met.

1.2 Contributions of thesis

The work presented in this thesis is a continuation of previous projects documented in [Bengtsson, 2004; Strandh, 2006]. These previous projects focused on control of combustion phasing in a pure HCCI engine using port injection of fuel and running on laboratory fuels ethanol and n-heptane. The focus of the present project is to build on previous results and merge these into more commercially viable engine configurations. The engine has therefore been rebuilt for direct injection of diesel fuel into the cylinders.

The work has been performed in close collaboration with Kent Ekholm at the Department of Energy Sciences at Lund University. The

author has been responsible for the majority of the work on control design and control system development. Experimental planning and experimental work has been done in collaboration with Kent Ekholm.

The first part of the work presented here was performed on the original engine set-up with port-injected fuel only. One limitation in previous work on combustion phasing control in HCCI engines is saturation of the chosen actuator, such that the given reference value for combustion phasing cannot be held over the desired operating range. A solution to this problem was found by combining two actuators, inlet valve closing (IVC) and exhaust gas recirculation (EGR), in a mid-ranging control structure specifically designed for two-input-one-output systems.

In the second part of the work, the engine was operated using a combination of the two fuel injection systems, known as fumigation operation. With ethanol used for the port-injected fuel and diesel for the direct-injected fuel, much freedom was obtained to influence combustion. It was shown that the engine could be operated safely this way with HCCI-like emissions at medium-to-full load. At the higher loads, the combustion became extremely sensitive to fuel injection settings, and a control system was necessary to be able to perform these experiments.

The third part of the work was performed using direct-injection only. The distinction between traditional diesel combustion and diesel-HCCI combustion is not sharp in this case, and mainly a matter of the degree of homogeneity of fuel-air mixture at the time of ignition. Two factors that influence homogeneity are injection timings and EGR rate. For this type of combustion, there is a clear NO_x-soot trade-off, and the main idea in this work was to minimize a weighted sum of NO_x and soot using injection timings and EGR valve position as control variables.

The thesis starts with a background presentation of key engine parameters and previous work on low-emission engine concepts in Chapter 2. The equipment used throughout the experiments is then introduced in Chapter 3. Then follows the presentation of the three main contributions on port-fuel injection HCCI, fumigation, and direct-injection diesel operation in Chapters 4, 5, and 6, respectively. These chapters present the methods and results of the three separate parts of the work, whereas conclusions and directions for future work are presented in Chapter 7 in order to relate and contrast the different

parts of the thesis. A list of symbols and acronyms is included at the end of the thesis.

1.3 Publications

The thesis is based on the following publications:

Karlsson, M., K. Ekholm, P. Strandh, R. Johansson, P. Tunestål, and B. Johansson (2007): "Closed-loop Control of Combustion Phasing in an HCCI Engine Using VVA and Variable EGR". In *Proc. for the Fifth IFAC Symposium on Advances in Automotive Control*, pp. 517–524. Aptos, CA, USA.

Ekholm, K., M. Karlsson, P. Tunestål, R. Johansson, B. Johansson, and P. Strandh (2008): "Ethanol-Diesel Fumigation in a Multi-Cylinder Engine". *SAE Technical Paper 2008-01-0033*.

Karlsson, M., P. Strandh, K. Ekholm, R. Johansson, and P. Tunestål (2008): "LQG Control for Minimization of Emissions in a Diesel Engine". Submitted to *IEEE Multi-conference on Systems and Control*. San Antonio, TX, USA.

Other relevant publications:

Haugwitz, S., M. Karlsson, S. Velut, and P. Hagander (2005): "Anti-windup in Mid-ranging Control". In *Proc. of the European Control Conference and the Conference on Decision and Control*, pp. 7570–7575. Seville, Spain.

Blom, D., M. Karlsson, K. Ekholm, P. Tunestål, and R. Johansson (2008): "HCCI Engine Modeling and Control Using Conservation Principles". *SAE Technical Paper 2008-01-0789*.

2

Background

This chapter presents background information on low-emission engine concepts and the control challenges associated with such engines.

2.1 Low-emission engine concepts

Engine emission characteristics

Regulated emissions for automotive engines are hydrocarbons (HC), carbon monoxide (CO), oxides of nitrogen NO_x, and particulate matter (PM). In diesel engines, HC and CO emissions are low because the engine is always operated lean, i.e., with excess of oxygen, and fuel is not in contact with cylinder surfaces [Heywood, 1988].

NO_x and PM emissions are however significant in diesel engine combustion. NO_x is a common notation for NO and NO_2, but under normal engine conditions, formation of NO dominates over NO_2. The main part of NO is formed as so called thermal NO, where formation can be modelled by the extended Zeldovich mechanism consisting of three chain reactions [Heywood, 1988]

$$\begin{aligned} O + N_2 &\Leftrightarrow NO + N \\ N + O_2 &\Leftrightarrow NO + O \\ N + OH &\Leftrightarrow NO + H. \end{aligned} \tag{2.1}$$

Taking into account the chemical kinetics rate constants, the kinetics can be simplified by assuming equilibrium concentrations of certain

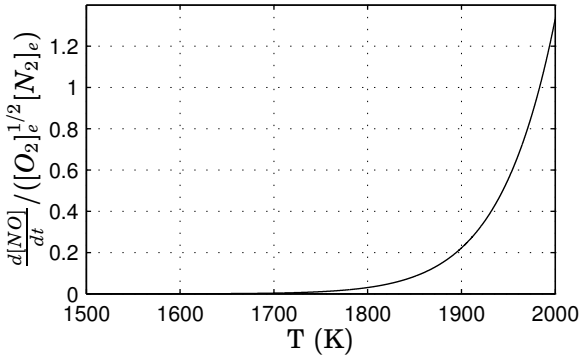

Figure 2.1 Initial formation rate of NO from Zeldovich mechanism, normalized by species concentration expression $[O_2]_e^{1/2}[N_2]_e$.

species which yields an expression for the initial NO formation rate given in mol/(cm^{3}s)

$$\frac{d[NO]}{dt} = \frac{k_1}{T^{1/2}} \exp\left(\frac{-k_2}{T}\right) [O_2]_e^{1/2}[N_2]_e \tag{2.2}$$

where $k_1 = 6 \cdot 10^{16}$ s(Kmol/cm^3)$^{1/2}$, $k_2 = 69090$ K, and $[O_2]_2$ and $[N_2]_e$ denote equilibrium concentrations. Formation rate is strongly dependent upon temperature, as can be seen in Figure 2.1 where the formation rate is plotted normalized by the species concentration expression $[O_2]_e^{1/2}[N_2]_e$.

From (2.2), it can be deduced that three factors are required for any significant NO formation to occur: high temperature, air, and sufficient time for the reaction to proceed. In [Dec, 1997], a number of studies on diesel combustion using different optical techniques are condensed into a phenomenological model of the diesel engine combustion process. The studies indicate that NO is mainly formed in the diffusion flame around the fuel jet periphery and in the hot gas regions that remain at the end of combustion. At these locations, all three conditions for NO formation are fulfilled.

Particulate matter from diesel engines consists mainly of soot which is carbonaceous particles on which organic molecules may be absorbed.

Soot formation is governed by the processes of particle formation, where small nuclei of hydrocarbons with a low H/C ratio are formed where combustion is locally very rich, and particle growth where these nuclei aggregate and adsorb smaller particles to the surfaces. When the soot particles come in contact with oxygen at sufficiently high temperature, they oxidize to form CO_2 or CO [Heywood, 1988]. Conditions required for PM formation are thus combustion with a locally rich mixture, sufficient time for particle growth, and for the particles to avoid entering zones where they may be oxidized.

In [Dec, 1997], it was concluded that soot is formed throughout the fuel jet cross section but the major part of soot formed is oxidized within the cylinder. Soot that does not oxidize and ends up as PM emissions is thought to be formed mainly during the end of fuel injection and after injection stops. Injection pressure drops towards the end of injection, resulting in poorer atomization of fuel and thus poorer mixing of fuel and air leading to more fuel being burned in very rich zones. Additionally, the soot particles formed from the last fuel injected during the cycle will have less time to oxidize within the cylinder, and the cylinder temperature late during the expansion stroke may be too low for oxidation to occur.

The high NO_x and PM emission levels from diesel engines are further complicated by the fact that aftertreatment of these emissions is difficult. Since the engine is operated lean, reduction of NO_x in a three-way catalyst is not possible. To comply with emissions standards introduced in 2006–2008, aftertreatment of NO_x is currently being implemented commercially based on selective catalytic reduction (SCR) [Volvo Group, 2004]. The principle behind SCR technology is to reduce NO_x to N_2 with the aid of a catalyst by injecting a reducing agent, typically urea, into the exhaust gases [Turns, 2000]. SCR aftertreatment is costly; the production cost has been estimated at $1200–$3200 per new vehicle [Environmental Protection Agency, 2001], and to that should be added maintenance costs as well as operational costs for refilling urea.

Particulate filters, also known as particulate traps, can be used to oxidize a significant part of the engine-out PM. Because the oxidation efficiencies of these filters cannot reach 100 %, engine-out PM emissions must still be sufficiently low to make tailpipe emissions comply with legislation.

The HCCI engine

To reduce engine-out emissions of NO_x, it can be concluded from the previous discussion that the maximum temperature in the cylinder during the combustion process should be reduced. To reduce PM emissions, combustion in zones that are locally very rich should be avoided. A way to simultaneously reduce NO_x and PM emissions is to replace the inhomogeneous diffusion combustion of the diesel fuel jet with combustion of a homogeneous, lean mixture of fuel and air. With a homogeneous combustion of a homogeneous mixture, temperature is approximately homogeneous over the cylinder. With a homogeneous temperature, zones with very high temperature are eliminated so that the maximum temperature is reduced to a value below which no significant NO_x formation occurs. Also, with a lean homogeneous mixture there will be no locally rich zones that contribute to PM formation.

Homogeneous charge compression ignition (HCCI) was first studied in the '70s [Onishi *et al.*, 1979; Noguchi *et al.*, 1979] for two-stroke engines where the combustion concept was shown to reduce emissions, improve fuel economy and reduce cyclic variability. The concept was later transferred to four-stroke engines [Najt and Foster, 1983; Thring, 1989]. These early four-stroke papers advocated the HCCI engine for its potential to combine CI efficiencies with SI power densities. With the increased focus on emissions in the '90s, publications a decade later focus heavily on the potential excellent emission characteristics of the HCCI concept [Ryan and Callahan, 1996; Aoyama *et al.*, 1996].

The HCCI concept is based on auto-ignition of a homogeneous fuel-air mixture. For the mixture to be homogeneous at the time of ignition, there must be sufficient time available for the fuel and air to mix. This can be accomplished either by injecting the fuel into the inlet port and thus let air and fuel mix before entering the cylinder, called port fuel injection (PFI), or injecting it directly into the cylinder early enough to allow for mixing before autoignition.

In order for the lean mixture to auto-ignite, temperature must be sufficiently high. Depending on the fuel, the temperature requirements are different. With high octane-number fuels that do not auto-ignite easily, such as gasoline or ethanol, preheating of the mixture in the intake or high levels of internal residuals (hot gases retained in cylinder from one cycle to next) is required. With low octane-number fuels, such

as diesel, sufficient temperature for auto-ignition may not be an issue but the temperature must still be high enough for the fuel to vaporize. For maximum efficiency, the mixture should auto-ignite close to top dead center (TDC).

Another key aspect in making HCCI combustion feasible is to limit the heat release rate once combustion has started. Very rapid heat release causes high in-cylinder pressures and rapid pressure changes that may damage the engine and lead to unacceptable levels of audible noise. Heat release rate depends on combustion phasing, i.e., the time during the engine cycle where combustion occurs, and the dilution of the mixture. There are two principal ways of diluting the mixture, either by making the mixture leaner through excess air, or by using exhaust gas recirculation (EGR).

The two requirements on ensuring that the mixture auto-ignite, and on limiting the heat release rate are to a large extent opposing each other [Zhao and Asmus, 2003]. With higher temperatures, the mixture will auto-ignite more easily but also demonstrate a more rapid combustion. High dilution may limit the heat release rate to acceptable levels, but also requires higher temperatures for auto-ignition. A major current limitation of the HCCI concept is that the operating range is restricted to medium-load and limited by temperature requirements to avoid misfire at low load and dilution capacity at high load. To put the HCCI concept into production, it is essential that the engine can operate in dual-mode, i.e., switch to traditional SI or diesel engine operation at low and/or high loads [Zhao and Asmus, 2003].

Low temperature combustion diesel engines

HCCI research using diesel fuel has mainly focused on direct-injection of fuel into the cylinder [Zhao and Asmus, 2003]. The basic engine set-up is then in principle identical to a traditional diesel engine which facilitates mode switching at high or low loads. In pure HCCI operation, the fuel-air mixture should be completely premixed at the time of auto-ignition whereas in traditional diesel combustion, the grand majority of the fuel burns in a diffusion flame. Between these two extremes, there is a range of combustion modes varying with respect to the homogeneity of fuel and air both spatially throughout the cylinder and temporally throughout the combustion process.

Because the difference between premixed and diffusion flame com-

bustion is not sharp for such engine set-ups, nomenclature is somewhat unclear. Depending on the set-up and the degree of homogeneity, the combustion mode has been referred to by different names, e.g., PREDIC (premixed lean diesel combustion) [Takeda *et al.*, 1996], PCI (premixed compression ignited) [Iwabuchi *et al.*, 1999], MK (modulated kinetics) [Kimura *et al.*, 1999], and PPC (partially premixed combustion) [Noehre *et al.*, 2006; Lewander *et al.*, 2008]. The set-ups differ in terms of injection strategy (injection timings, injection pressure, multiple injections), injector design, EGR rate, combustion chamber geometry, compression ratio, etc. Common issues in these set-ups are to avoid over-penetration of liquid fuel causing wall wetting and high HC emissions, to balance NO_x and soot emissions, and to retain diesel-like efficiencies.

Musculus [Musculus, 2006] performed a similar study to [Dec, 1997] for early-injection, high-EGR, low temperature diesel combustion. The optical studies show that compared to traditional diesel combustion, liquid fuel penetrates further into the combustion chamber. Also, combustion occurs throughout the fuel jet cross section indicating a premixed combustion process of a locally lean mixture. Soot is formed further downstream compared to traditional diesel combustion, at the head of the fuel jet.

For traditional diesel combustion, there is a clear NO_x-soot trade-off [Heywood, 1988]. High levels of EGR or late combustion phasing reduces in-cylinder temperature which leads to reduced NO_x-formation according to Figure 2.1, but at the same time, reduced temperature inhibits oxidation of soot. Though, for very high EGR rates, temperature drops below a threshold under which no soot is formed so that simultaneous reduction of NO_x and soot is possible [Akihama *et al.*, 2001; Noehre *et al.*, 2006]. Figure 2.2 shows soot, NO_x, and the overall engine efficiency, called the brake efficiency, for constant injection timing at 12° BTDC. It can be seen that for very high EGR rates both NO_x and soot emissions are low, as is brake efficiency. For lower EGR rates, there is a clear NO_x-soot trade-off.

In-cylinder emissions reduction in diesel engines based on reducing combustion temperature using EGR combined with advanced injection strategies is currently being implemented commercially as an alternative to aftertreatment systems [Scania, 2006].

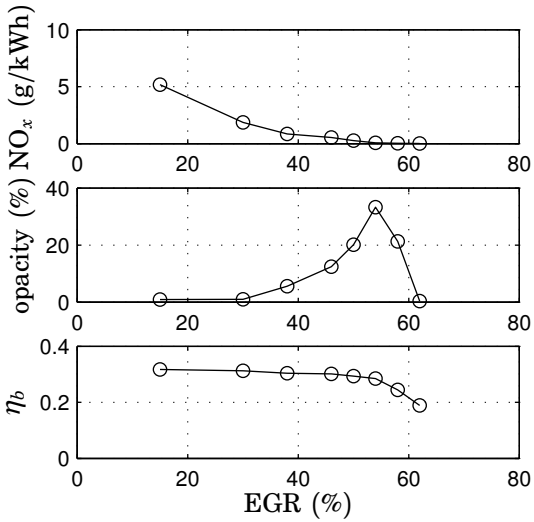

Figure 2.2 NO_x, soot, and brake efficiency for varying EGR rate at a fixed injection timing of 12° BTDC.

2.2 Control challenges

The low-emission engine concepts presented in the previous section are inherently more difficult to control as compared to conventional SI or diesel engines. In SI engines, the combustion process is controlled by the spark, and in diesel engines by the fuel injection. Both HCCI and low temperature diesel combustion rely on forming a largely homogeneous fuel-air mixture prior to auto-ignition, but there is no direct trigger of the start of combustion. In any type of engine it is important to have a stable, predictable combustion process. Too early or too late combustion phasing results in bad efficiency, bad emissions characterstics, or potential damage to the engine.

There are many variables influencing the combustion process, such as engine speed, load, temperature, age, etc. To maintain advantageous combustion process characteristics as these variables change, the engine must be equipped with some measure to counteract the variations.

Possible actuators are injection timings, injection pressure, EGR rate, turbo boost, valve timings, etc.

Open-loop versus closed-loop control

In practice, there are two fundamental classes of control solutions – open-loop and closed-loop control. Open-loop control strategies are common in engine applications [Guzzella and Amstutz, 1998], where control variables are mapped according to operating conditions such as speed and load. Calibrating such maps for optimal performance is a huge effort which increases as requirements get tighter and more degrees of freedom are added to the engine. Optimizing maps for steady-state operation may be challenging enough, but process dynamics makes optimizing transient behavior even more difficult. Another limitation of the open-loop approach is that it does not take changes in engine behavior due to wear into consideration.

Closed-loop control uses measured information from the combustion process to determine actuator settings. The obvious drawback is the reliance upon sensors which in general are expensive to install in production engines and may fail during operation. Certain indirect sensors, such as pressure and temperature sensors are already available in production, but so far sensors that give direct information on the combustion process in each individual cycle are only used in laboratory settings.

The purpose of control may be different depending on the application. One purpose is to stabilize an unstable process. Instabilities may arise e.g. at high load in HCCI engines where interactions between combustion timing and cylinder wall temperatures create a positive feedback loop that needs to be stabilized by closed-loop control [Olsson *et al.*, 2002]. Another purpose is to counteract disturbances such as varying load, speed, etc. so as to maintain advantageous conditions for combustion. Open-loop control is often successfully used to handle this control problem, but depending on the requirements and the process closed-loop control may be necessary. Yet another purpose of control is process optimization. With tight requirements on the combustion process to comply with emissions legislation and to keep high engine efficiency, a two-level control structure may be required. A high-level loop determines optimal setpoints for measured variables such as combustion phasing, and a low-level control loop adjusts actuator settings

to keep the measured variables at these setpoints. Examples of control structures aimed at addressing control problems from all three categories are included in this thesis.

In-cylinder pressure sensor feedback

The work presented in this thesis focuses on benefits of closed-loop control based on in-cylinder pressure sensors. An example of cylinder pressure measurements during a cycle from one of the cylinders is shown in the upper plot in Figure 2.3. From the cylinder pressure measurement, also known as the pressure trace, a simplified rate of heat release computation is performed, according to [Heywood, 1988]

$$\frac{dQ}{d\theta} = \frac{\gamma}{1-\gamma} p(\theta) \frac{dV}{d\theta} + \frac{1}{\gamma - 1} V(\theta) \frac{dp}{d\theta}. \tag{2.3}$$

This simplified rate of heat release assumes the cylinder mixture to be an ideal gas with a constant ratio of specific heats γ, and does not consider mass transfer to and from crevices or heat transfer to and from walls. The cumulative heat released Q is shown in the middle plot in Figure 2.3. The instantaneous heat release rate $dQ/d\theta$ is generally heavily corrupted by noise if computed directly from (2.3). Heat release rates that are shown in this thesis are therefore low-pass filtered using a Hamming window of width ± 1 CAD, see the lower plot in Figure 2.3.

From the pressure trace and heat release rate, parameters characterizing the combustion process can be computed. In this thesis, the parameters α_{10} and α_{50} representing the crank angle degree of 10% and 50% heat released are used. In general, α_x is defined by

$$100 \cdot \frac{Q(\alpha_x)}{\max_\theta Q(\theta)} = x.$$

Two other parameters are used that are computed from cylinder pressure measurements, the maximum pressure derivative d_p,

$$d_p = \max_\theta \frac{dp}{d\theta},$$

and the net indicated mean effective pressure defined as

$$\mathrm{IMEP}_n = \frac{1}{V_D} \int p dV,$$

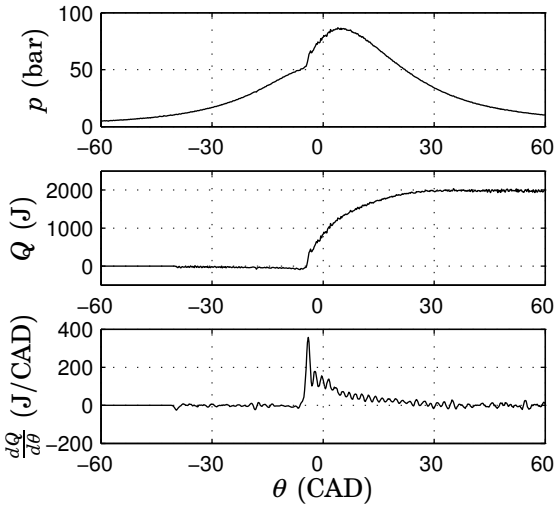

Figure 2.3 Cylinder pressure measurement for one cycle (top), cumulative heat released (middle), and low-pass filtered instantaneous heat release rate (bottom).

where the integral is computed over an entire engine cycle. IMEP_n is a measure of work produced during an engine cycle, normalized by the displaced volume.

Cylinder pressure sensors cannot yet be incorporated into production engines due to cost and durability concerns. Thus, the results are so far only applicable in laboratory settings, but it is likely that sensor development will eventually result in a cheap reliable sensor that can provide information on the same combustion parameters that are here extracted from the cylinder pressure trace.

3

Experimental set-up

Engine specifications

All experiments were performed on a Volvo D12 six-cylinder heavy-duty engine, see Figure 3.1. The engine has been used in previous projects, see [Bengtsson, 2004; Strandh, 2006]. Within the current project, the engine has been equipped with a direct injection system, actuated valves for EGR and VGT control, and a fuel injection pressure sensor. Additionally, significant work has been devoted to extending the capabilities of the control system.

The geometrical engine specifications are given in Table 3.1. The engine speed was governed by an ABB electrical motor with a rated power of 355 kW.

Actuators

Several variables could be directly actuated from the control system software. Cylinder-individual actuation was available for port-fuel injection of two different fuels, direct injection fuel injection timing, injection duration, injection pressure, and crank angle degree of inlet valve closing. Actuated variables common to all cylinders were inlet air heating, the position of an EGR valve, an exhaust back pressure (EBP) valve, and a variable geometry turbo (VGT) valve.

Port fuel injection Two injectors were mounted upstream of the inlet port of each cylinder. The fuels used were ethanol and n-heptane. The injectors opened once every engine cycle, and the amount of fuel

Table 3.1 Engine specifications.

Operated cylinders	6
Total displaced volume	12.2 dm^3
Bore	131 mm
Stroke	150 mm
Connecting rod length	260 mm
Valves per cylinder	4
Compression ratio	18.5:1

injected was controlled by varying the injection duration. The twelve injectors were controlled from the computer using fiber optic cables to one PIC (peripheral interface controller) processor for each injector.

Direct injection Standard production unit injectors from Delphi were used for direct injection. The embedded software was modified to

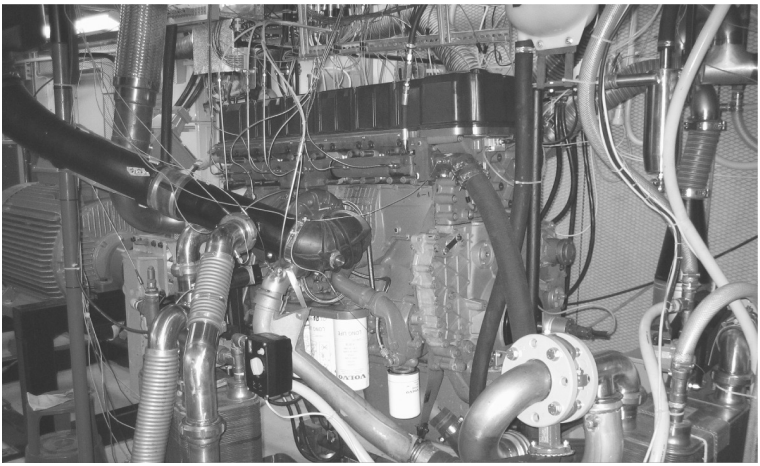

Figure 3.1 Engine used in experiments.

Table 3.2 Valve timings.

Valve event	Timing (CAD ATDC)
IVO	340
EVO	101
EVC	381

allow start of injection, injection duration, and fuel injection pressure to be set from the computer using CAN communication.

Variable valve actuation The VVA system was a commercial, research-type electro-hydraulic system. The system was driven by the cam shaft and allowed for valve closings ahead of the cam curve, a so-called *lost motion system*. A hydraulic cylinder was used to move the inlet valve. Oil was transferred to this cylinder from another hydraulic cylinder either by an electronically controlled valve or by the cam shaft pushing on the second cylinder. Hence, valve closings ahead of the cam curve, but not after was possible. PIC processors were used, analogously to the port fuel injection system.

Only IVC actuation was used in the experiments, the other valve timings are given in Table 3.2

Inlet air heater An electrical heater with a capacity of 35 kW was used to control the temperature of the inlet air. A PI-controller was used to set the heater power from a reference inlet temperature and the measured temperature. If no inlet air heating was desired, two valves could be shifted such that the air instead passed through an intercooler.

Gas path valves Two valves, the EGR and EBP valves, were used to control the EGR rate in the engine, see Figure 3.2. Servo motors from JVL Industri Elektronik A/S were used to actuate the valves. The servo motors were controlled from the computer using serial communication.

The same type of actuated valve was used to manipulate the boost pressure using the VGT.

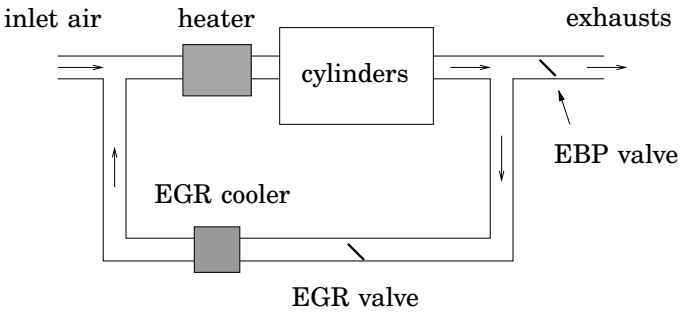

Figure 3.2 The EGR system.

Sensors

Cylinder pressure Piezo-electrical, water-cooled pressure transducers of type Kistler 7061B were used to measure the cylinder pressure. The transducers had a calibrated pressure range of 0–250 bar. Cylinder pressure measurements were collected every 0.2 CAD, and sampling was controlled by an engine crank sensor in the form an incremental encoder from Leine & Lindes.

Fuel injection pressure Diesel injection pressure was measured for cylinder 1, with the same resolution of 0.2 CAD as the cylinder pressure. The sensor was a strain gauge mounted on the rocker arm.

Other pressure sensors Pressure transducers for measuring pressure outside the cylinder were used for

- pressure after compressor
- inlet manifold pressure
- outlet pressure for cylinders 1,2,3
- outlet pressure for cylinders 4,5,6
- pressure after turbine
- oil pressure

- fuel pressure for port-injected fuels
- diesel pressure

The sensors were of type Keller PAA-21S, and had measurement ranges of either 0–5 bar or 0–10 bar.

Temperature sensors Temperature sensors were used for

- temperature after compressor
- temperature before heater
- intercooler temperature
- temperature after intercooler
- temperature after heater
- inlet manifold temperature
- individual exhaust temperatures from the six cylinders
- temperature after turbine
- EGR cooler temperature
- temperature after EGR cooler
- cooling water temperature
- oil temperature
- fuel temperature for port-injected fuels
- diesel temperature

Thermocouples of type K from Pentronic were used as temperature sensors.

Fuel flow measurements Fuel consumption was computed from scale measurements of fuel weight. An AVL fuel balance was used for diesel weight measurement, and scales from Sartorius for weight measurements of the port injected fuels.

Torque sensor A torque sensor mounted on the electrical motor measured the engine torque.

Emissions measurements The emissions measurement instrumentation was compiled by Boo Instrument AB. Hydrocarbons were measured using a flame ionization detector from JUM Engineering. NO_x were measured using a chemiluminescence detector from Eco Physics. CO and CO_2 were measured using a non-dispersive infrared detector, and oxygen concentration was measured using an oxygen paramagnetic attraction device, both from SICK-MAIHAK. Soot was measured using an opacimeter from SwRI.

Control system

Hardware A standard PC with a 2.4 GHz Pentium 4 processor was used to run the engine control system.

A Microstar DAP 5400a/627 parallel sampled data acquisition card was used for cycle-to-cycle data collection of cylinder pressures, fuel injection pressure, and fast sampling of inlet manifold temperature and pressure, engine speed, and temperature before heater. The card had 16 analog inputs and eight 1.25 MHz AD-converters with 14 bits resolution. Whenever one cylinder passed EVO, data were transferred from the card to the main program.

A National instruments NI6014 card was used to actuate the voltage level for the intake air electrical heater.

A PCIcanX II card from Kvaser was used for communication with diesel injectors.

A HP 3852A data logger was used to sample temperatures, pressures, fuel weights, and engine torque with a sampling rate of 0.4 Hz. The logger also actuated the voltage level to the intercooler and the EGR cooler.

Software The operating system used was the Linux distribution Fedora Core 6. The main engine control program was written in C++. Multiple threads in the program provided good real-time properties with robust cycle-to-cycle cylinder-individual actuation.

The graphical user interface was designed and saved as XML-code using `Glade`, and then converted to C++-code using `gtkmm`. The code was then compiled into a separate program so as not to interfere with the engine control system. The graphical user interface is shown in Figure 3.3.

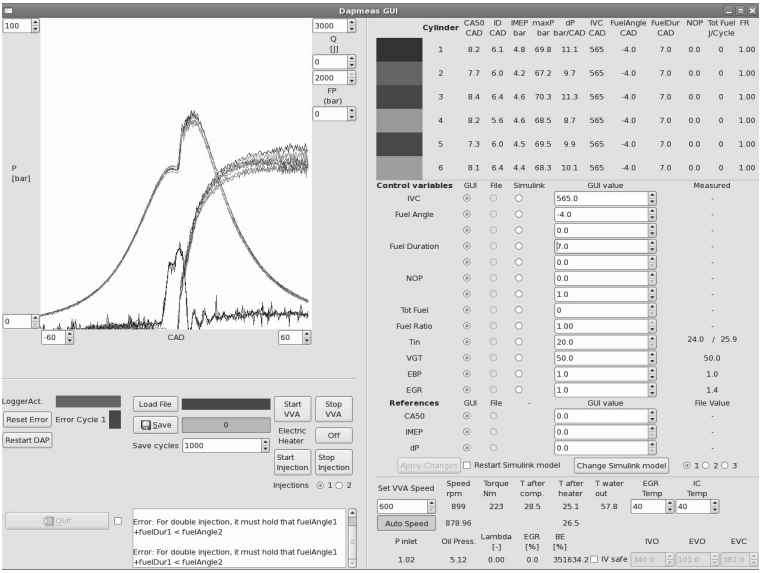

Figure 3.3 Graphical user interface.

Controllers were designed using Simulink and converted to C-code using Real Time Workshop. The C-code was then compiled to an executable program which communicated with the main program using FIFO pipes.

The combined system made it easy to change both control structure, controller parameters, actuated variables, and controlled variables while the engine was running.

4

Control of port-fuel injection HCCI operation

4.1 The combustion phasing control problem

Combustion phasing control is a large area of interest within HCCI engine research [Zhao and Asmus, 2003]. As mentioned previously, the reason is the lack of a direct combustion trigger such as spark or fuel injection timing. Once combustion starts in an HCCI engine it is rapid, which could lead to excessive in-cylinder pressures or pressure derivatives. The phasing of the rapid combustion event must therefore be carefully controlled within the cycle to avoid too early combustion that leads to high pressures or too late combustion that leads to low brake efficiencies, high levels of HC and CO emissions, and the risk of misfire. A consequence of the lack of a direct combustion trigger is also that combustion phasing becomes very sensitive to disturbances such as variations in speed, load, and engine temperature.

Combustion phasing constitutes a dynamical system due to interactions with cylinder wall temperatures. Early combustion phasing leads to high in-cylinder temperatures thus increasing heat transfer to the walls, and high wall temperatures lead to earlier combustion phasing. At high loads, it has been shown that the combustion phasing dynamics can become unstable [Olsson *et al.*, 2002]. At lower loads, the dynamics are stable but sensitive to operating conditions.

Various actuator options have been suggested to control combustion phasing which is here quantified by α_{50}. In dual-fuel actuation, the ratio of two fuels with different auto-ignition properties is varied [Olsson *et al.*, 2001; Strandh *et al.*, 2004]. In variable valve actuation (VVA), the crank angle degrees of inlet and exhaust valve openings and closings are varied. Variable valve timings affect the effective compression ratio, and thus the time of auto-ignition. Different set-ups are possible where some valve timings are fixed and others are varied, e.g., variable inlet valve closing (IVC) [Agrell *et al.*, 2003; Strandh *et al.*, 2005]. Variable valve actuation can influence the combustion process in more than one way; inlet valve closing can be used to alter the effective compression ratio, and exhaust valve timings can be used to manipulate the amount of residual gases in the cylinder from one cycle to next [Shaver *et al.*, 2006]. Other actuator options for combustion phasing control are variable compression ratio (VCR) [Haraldsson *et al.*, 2002], or fast thermal management [Martinez-Frias *et al.*, 2000].

In multi-cylinder engines, cylinder-individual actuation is required since thermodynamic conditions may vary greatly between cylinders. All the previously mentioned actuation options can be made cylinder-individual with appropriate hardware. Other means of influencing combustion phasing may have to be common to all cylinders. Such actuation options include variable exhaust gas recirculation (EGR) or variable inlet temperature if a common heater is to be used for the inlet air to all cylinders.

Independent of which actuator option that is chosen, actuator saturation will limit the operating range in HCCI mode by not providing enough energy to the fuel-air mixture for auto-ignition at low loads, and not being able to limit the heat release sufficiently at high loads. It is therefore of interest to study combinations of actuators to improve the capacity to adapt to operating conditions and thus extending the HCCI operating range.

This work focuses on combining variable IVC and variable EGR to control combustion phasing over a larger operating range than is possible using variable IVC alone. The set-up of combining these two control variables was first suggested as a topic of future work in [Agrell *et al.*, 2003], and elaborated upon in [Agrell and Linderyd, 2005]. In that work, no specific control structure or control design approach was suggested, and multi-cylinder engine issues were not treated explic-

itly. The publication [Karlsson *et al.*, 2007] was the first experimental verification of successfully combined IVC and external EGR actuation.

4.2 Experimental conditions

The port-fuel injectors in the intake to each cylinder were used for fuel-injection, with one injector used for ethanol and the other for n-heptane. The fuel energy ratio was fixed to 75 % ethanol and 25 % n-heptane. The electric inlet air heater maintained the inlet air temperature at 120°C. The exhaust valve timings as well as inlet valve opening were kept constant at the default values given in Chapter 3.

Two actuator variables were used, inlet valve closing u_{IVC} given in crank angle degrees after combustion top dead center, and the position of the EBP valve u_{EGR}. The control objective was to control α_{50}.

IVC actuation

The steady-state effect of u_{IVC} on α_{50} is shown in Figure 4.1. With changed inlet valve closing, the effective compression ratio of the engine changes, and thus the combustion phasing. It can be seen that the same α_{50} can be obtained by closing the inlet valve either during the expansion stroke before bottom dead center, or during the compression stroke after bottom dead center. Here, only closing after bottom dead center was applied.

A step response from u_{IVC} to α_{50} is shown in Figure 4.2. The effect on α_{50} from a change in u_{IVC} is almost immediate. A slow trend of gradually increasing α_{50} after the step in u_{IVC} could be discerned in the figure which is conjectured to be caused by wall temperature effects.

EGR actuation

The two valves marked EGR and EBP in Figure 3.2 control the EGR flow. In this work, the EGR valve was kept fully open and the control variable u_{EGR} represents the position of the EBP valve. The value of $u_{EGR} = 0$ corresponds to a fully open valve and $u_{EGR} = 100$ to a fully closed valve.

In Figure 4.3, the steady-state effect of the valve position u_{EGR} on α_{50} at engine speed $N = 1000$ rpm, $W_{in} = 1000$ J/cycle, and inlet

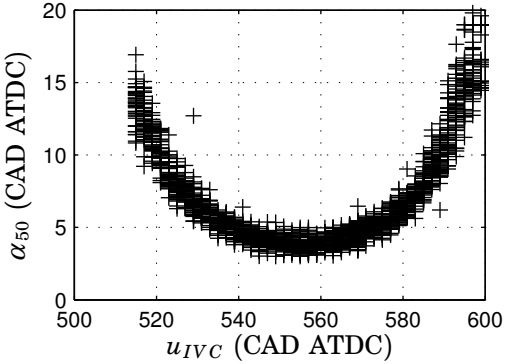

Figure 4.1 Steady-state relation between u_{IVC} and α_{50}.

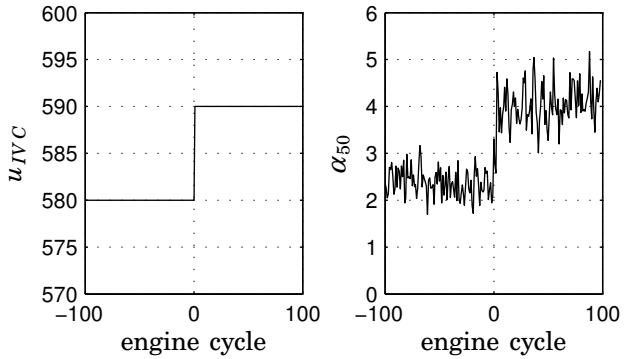

Figure 4.2 Step response from u_{IVC} to α_{50}.

valve closing $u_{IVC} = 560$ is shown. In general, a higher u_{EGR} leads to a higher concentration of CO_2 in the intake. The relationship between u_{EGR} and $[CO_2]$ is nonlinear whereas the relationship between intake $[CO_2]$ and α_{50} is fairly linear in the investigated interval. The nonlinearity thus appears to be caused by nonlinear effects of the valve and EGR path mass flow dynamics, e.g., pressure wave phenomena.

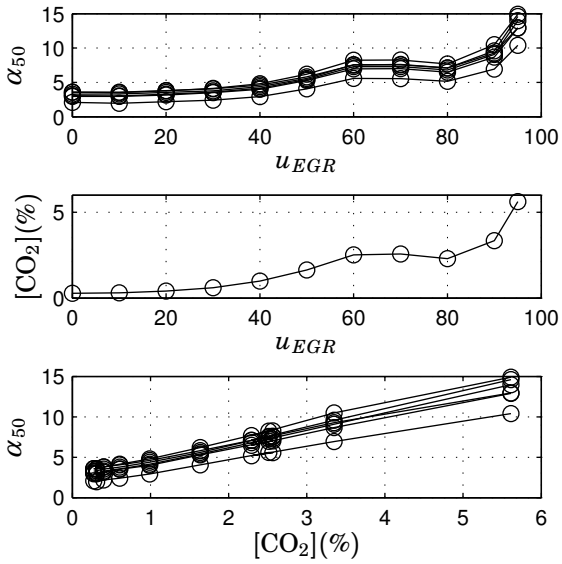

Figure 4.3 Measured steady-state relations between the valve position u_{EGR}, the CO_2 concentration in the intake, and the resulting α_{50} for the six cylinders.

A step response from u_{EGR} to α_{50} is shown in Figure 4.4. Because of dynamics in the EGR gas path, the effect of u_{EGR} on α_{50} is slow, compared to the effect of u_{IVC}.

Note that different operating conditions in terms of e.g. inlet temperature creates different offsets in α_{50} between the Figures 4.1, 4.2, 4.3, and 4.4.

4.3 Control design

Whereas both u_{IVC} and u_{EGR} can be used to control the combustion phasing α_{50}, the effects of these control variables are not identical. The input u_{IVC} is cylinder-individual whereas u_{EGR} is a scalar control variable that will affect the combustion phasing of all cylinders. While

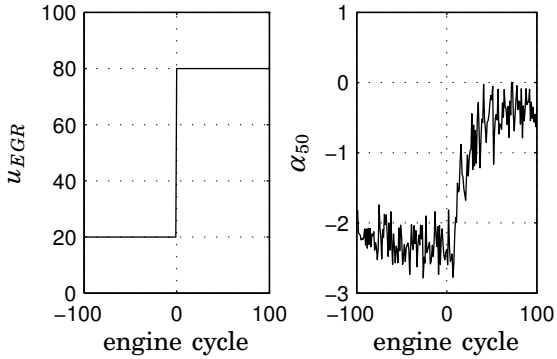

Figure 4.4 Step response from u_{EGR} to α_{50}.

the effect of u_{IVC} on α_{50} is almost immediate, the time constant from u_{EGR} to α_{50} is on the order of 30 engine cycles. To find a suitable control structure, the different characteristics of the two control variables, u_{IVC} and u_{EGR} must be taken into account and exploited.

Mid-ranging Control

Mid-ranging control is a control structure that is designed for processes with two control variables and only one process variable to control [Allison and Isaksson, 1998]. The key point is to combine a fast, accurate control variable with small operating range with a slow, less accurate control variable to extend the operating range. Mid-ranging control was first used in process control for the problem of controlling a flow using a small, fast and accurate valve and a large slower valve [Allison and Isaksson, 1998]. The problem of combining two control variables with different dynamic properties to control a single process variable arises in many applications. Mid-ranging control has therefore found use in many different fields, for an automotive application see [Solyom and Eriksson, 2006].

The structure of the basic mid-ranging controller is shown in Figure 4.5. In a first controller C_1, the fast input u_1 is used to control the process output y to its reference r. The second input u_2 is obtained from

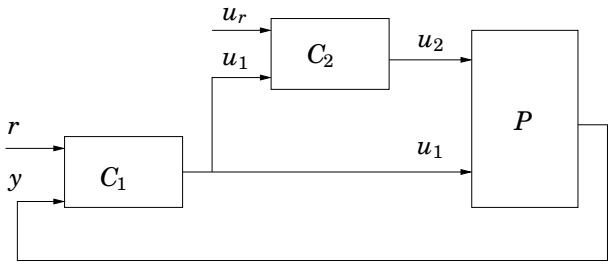

Figure 4.5 The basic mid-ranging control structure.

a second controller C_2 which controls u_1 to a reference u_r. The system ensures both a fast and accurate control of y through u_1 and prevents u_1 from permanently loosing control authority through saturation by adjusting u_2. The controllers C_1 and C_2 should be tuned according to the dynamic ranges of the corresponding control variables u_1 and u_2, which typically means that C_2 should have a lower bandwidth than C_1.

In principle, any type of controller could be used for C_1 and C_2. The most straightforward choice would be PID-controllers due to their ease of implementation and wide-spread use in industry. In [Allison and Isaksson, 1998], the mid-ranging control structure with PID-controllers is compared to model predictive control (MPC). The desired mid-ranging effect can be obtained by a suitably defined optimization criterion for the MPC controller. MPC has the advantage of explicitly handling constraints, but the disadvantage of greater complexity in terms of implementation and on-line computation.

A Control Structure for u_{IVC} and u_{EGR}

The task of using u_{IVC} and u_{EGR} to control α_{50} fits nicely into the mid-ranging control scheme with $u_1 = u_{IVC}$ and $u_2 = u_{EGR}$. With one cylinder only, the structure in Figure 4.5 could be immediately adopted. To handle a multi-cylinder engine, a modification is suggested where the n inlet valve closing signals $u_{IVC1} \dots u_{IVCn}$ are mapped into a single input to C_2 according to Figure 4.6.

The control structure leaves much freedom for design. The controllers C_1 and C_2, the references u_r, and the map $f(\cdot)$ can be chosen to achieve the desirable speed and robustness of the system. The func-

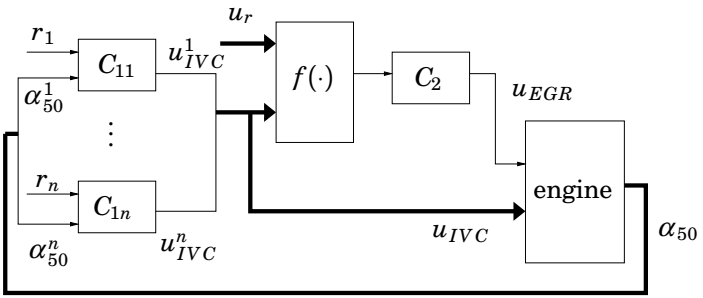

Figure 4.6 Control scheme for control using u_{IVC} and u_{EGR} for n-cylinder engine. Thick arrows represent vector signals.

tion $f(\cdot)$ should reflect how far u_{IVC} is from saturation. One choice may be

$$f(u_{IVC}, u_r) = \frac{1}{n}\sum_{i=1}^{n}(u_r^i - u_{IVC}^i),$$

where average deviation from the references u_r^i is computed. The references u_r^i should then lie in the middle of the operating range of u_{IVC}. In general, a common reference for all cylinders $u_r^i = u_{r0}$ would probably be appropriate, but for the sake of generality different references u_r^i are included here. Other options for $f(\cdot)$ are to increase the weighting of a signal when it saturates, such as in the map

$$f(u_{IVC}, u_r) = \frac{1}{n}\sum_{i=1}^{n}(u_r^i - u_{IVC}^i) + \frac{K_s}{n}\sum_{i=1}^{n}(\mathrm{sat}(u_{IVC}^i) - u_{IVC}^i),$$

where K_s is some positive constant, and the saturation function is defined as

$$\mathrm{sat}(x) = \begin{cases} x_{min}, & x \le x_{min} \\ x, & x_{min} < x < x_{max} \\ x_{max}, & x_{max} < x \end{cases},$$

or to only consider the maximum and minimum u_{IVC}^i, as in

$$f(u_{IVC}, u_r) = u_{r0} - \frac{\max(u_{IVC}) + \min(u_{IVC})}{2}.$$

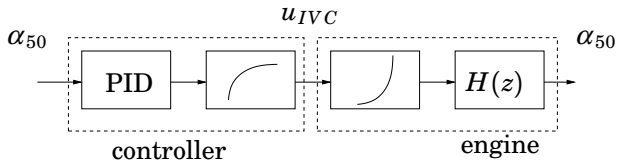

Figure 4.7 The structure of the controllers C_{1i} where a PID-controller is combined with the inverse of the process nonlinearity to achieve an approximately linear closed-loop system.

Handling Nonlinearities

The effect of u_{IVC} on α_{50} is nonlinear, as seen in steady-state in Figure 4.1. It is therefore difficult to find a standard linear PID-controller with satisfactory performance in a large operating range. Assuming that the nonlinear process can be modelled by a Hammerstein system, i.e., a static input nonlinearity in series with a linear dynamical system, a compensation for the nonlinearity can be included in the controllers $C_{11}, \ldots, C_{1n}$, as suggested in [Strandh *et al.*, 2005]. The output of the controller is transformed using the inverse of the estimated nonlinearity such that the system from the output of the PID-controller to the process output α_{50} is approximately linear, see Figure 4.7.

A similar compensation for the nonlinearity from u_{EGR} to α_{50} would be appropriate, but has not been included in the control system used in the experimental work presented here.

4.4 Results

The mid-ranging control structure was implemented in the engine control system. The controllers $C_1, \ldots, C_n$ for u_{IVC} were of PID-type and the controller C_2 for u_{EGR} of PI-type. The mapping $f(\cdot)$ from the vector u_{IVC} to the input of C_2 was chosen as

$$f(u_{IVC}, u_r) = u_{r0} - \frac{1}{6}\sum_{i=1}^{6} u_{IVC}^i,$$

which proved to work well in practice.

The inputs u_{IVC}^i were constrained to the range $u_{IVC}^i \in [568, 607]$ where the nonlinearity from u_{IVC} to α_{50} could be inverted in a robust way and the cycle-to-cycle variations were kept at an acceptable level at the tested operating condition. The reference for u_{IVC} was chosen as $u_r = 587$.

Step Responses at Constant Speed

In Figure 4.8 the results of an experiment where the EBP valve was fixed at $u_{EGR} = 45$ is shown. The engine speed was $N = 1000$ rpm and the total fuel energy $W_{in} = 1200$ J/cycle. It can be seen that there is a large difference among the cylinders when it comes to the u_{IVC} required to hold a constant α_{50}. These deviations arise from differences in termodynamic conditions; the cylinders located farthest from the heater will have a cooler mixture entering the cylinder and therefore a later combustion phasing for the same u_{IVC}. The temperature of the cooling water will also affect the combustion phasing. In the plot, we can see that taking this span into account, there is a very narrow operating range for u_{IVC}. For $\alpha_{50}^{ref} = 2$, u_{IVC} will saturate at its lower value for one cylinder, and at $\alpha_{50}^{ref} = 5$, u_{IVC} will saturate at its upper value for other cylinders.

Results from an experiment using the mid-ranging control structure are shown in Figure 4.9. The same values for speed, total fuel energy and fuel ratio as in Figure 4.8 are used. Here we can see the benefits of varying the EGR rate. When the reference value for α_{50} is increased, u_{IVC} is also increased and approaches its upper limit. The second controller then reacts and increases u_{EGR}, which means that a lower u_{IVC} is required to keep the reference value for α_{50}, and u_{IVC} is eventually reset to the middle of its operating range.

Speed Transients

An engine must be able to operate at a range of speeds and loads, not only in stationarity but also during transients. The variations in engine speed can be seen as a load disturbance and will have a large influence on combustion phasing. To test the performance of the control system during speed transients, experiments were performed with fuel energy $W_{in} = 1200$ J/cycle and engine speed varying from 1000 rpm to 1400 rpm.

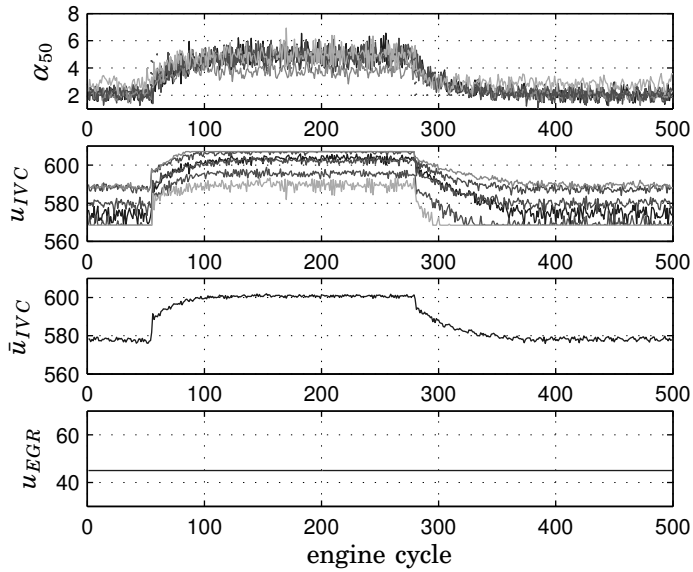

Figure 4.8 Step response experiment with constant u_{EGR}. In the upper two plots, α_{50} and u_{IVC} are shown for all six cylinders. The third plot shows the average of u_{IVC}.

In Figure 4.10, results are shown for the speed transient with constant u_{EGR}. It can be seen that u_{IVC} rapidly saturates at its lower value as the engine speed increases, and the reference $\alpha_{50}^{ref} = 4$ cannot be held. At 1400 rpm, combustion will then occur later than desired which may lead to reduced efficiency. At 1000 rpm, u_{IVC} saturates at its upper limit for some cylinder which causes too early combustion. Earlier combustion leads to higher in-cylinder pressures that may damage the engine. It can be concluded that the control variable u_{IVC} by itself cannot successfully control the combustion phasing, even for this modest variation in speed.

In Figure 4.11, results from a corresponding experiment with the mid-ranging control structure are shown. The combustion phasing α_{50} is kept at its reference α_{50}^{ref} throughout the experiment. The second

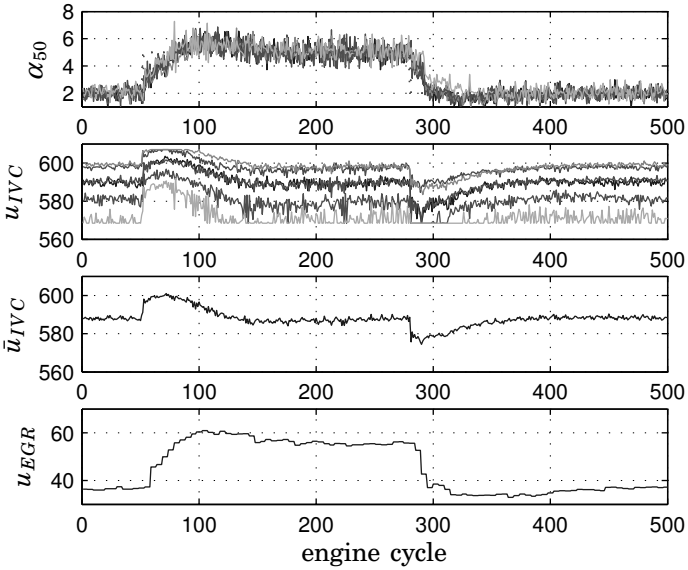

Figure 4.9 Step response experiment with the mid-ranging control structure.

control variable u_{EGR} adjusts so that u_{IVC} will remain within its operating range for all cylinders, making rapid cycle-to-cycle adjustments possible.

The effect of the nonlinearity from u_{EGR} to α_{50} shown in Figure 4.3 can be seen towards the end of this experiment. Here, u_{EGR} passes through the range $[60, 80]$ where the effect on α_{50} is small. Therefore, there is a delay in the reset of u_{IVC} which causes a small control error in α_{50} at engine cycles around 950. The error is eventually reset, but a compensation for the nonlinearity could improve performance.

From Figure 4.11, it could also be concluded that a static feedforward compensation from engine speed to α_{50} would not have resulted in satisfactory control. The speed is held constant at 1000 rpm both in the beginning and the end of this data set, but the value of u_{EGR} required to hold the reference α_{50} varies a great deal. The reason is that

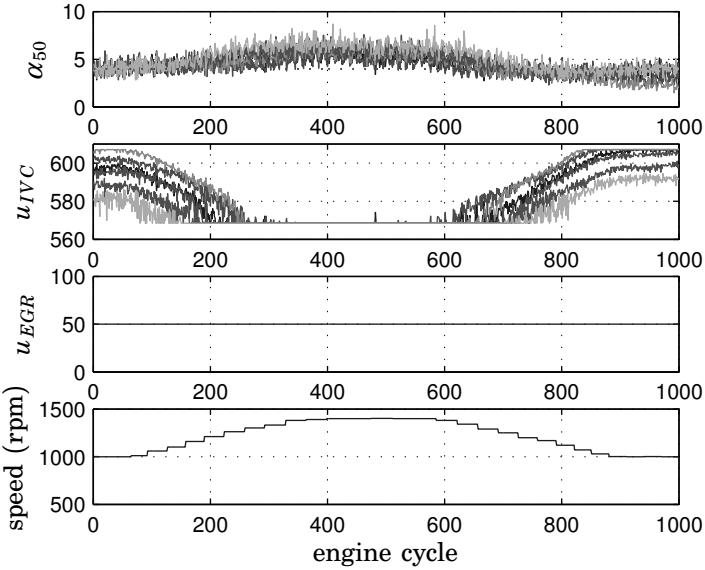

Figure 4.10 Speed transient with constant u_{EGR}. Increased engine speed retards the combustion phasing α_{50} which causes u_{IVC} to saturate for all cylinders such that the reference α_{50}^{ref} cannot be held.

the increase in speed from engine cycles 100 to 900 leads to increased wall heat transfer, and the heated walls lead to advanced combustion phasing that persists when speed is reset at the end of the transient.

The control system was also tested with variations in injected fuel energy. In the load range that was investigated, it was concluded that the load has only a small effect on the combustion phasing, and results were therefore similar for the mid-ranging controller as for a controller using u_{IVC} only.

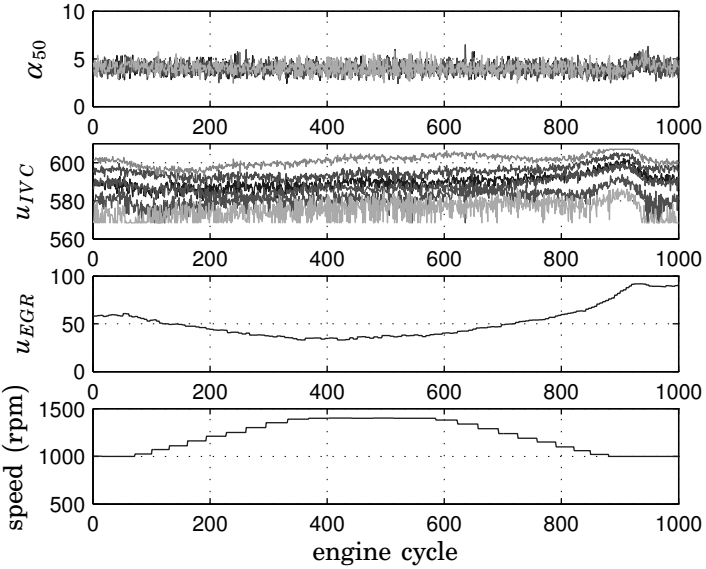

Figure 4.11 Speed transient with mid-ranging controller. By manipulating u_{EGR}, it is possible to keep u_{IVC} within its operating range during the entire speed transient so that α_{50} is kept at its reference value.

5

Control of fumigation operation

5.1 Fumigation

Fumigation is a form of dual-fuel engine operation where part of the fuel is premixed with the intake air, and part of the fuel is injected directly into the cylinder as in a traditional diesel engine. The premixed and direct-injected fuels may be of the same kind, or fuels with different properties may be used to achieve the desired mode of combustion. The two fuel injection systems give a large flexibility in influencing the combustion which implies that different combustion modes could be used in different parts of the operating range of the engine. There is thus a potential to combine the best features of port-fuel injection and direct injection to achieve low-emission combustion over a large operating range.

Various motivations to study fumigation have been presented. With low levels of premixed fuel, operation is close to that of a diesel engine. In this case, the introduction of the premixed fuel can reduce the ignition delay and pressure oscillations, ensuring a smoother operation at high loads [Zaidi *et al.*, 1998]. With diesel used for both the premixed and direct injected fuel, fumigation is a way of avoiding the knock problem associated with pure PFI diesel HCCI [Odaka *et al.*, 1999; Canova *et al.*, 2007]. With high levels of premixed high-octane number fuel,

engine operation is close to that of a spark ignition engine with the direct injected fuel replacing the spark [Kim *et al.*, 2004; Alger *et al.*, 2005]. With biogas as the premixed fuel and biodiesel as the direct injected fuel, this method has been presented as an engine concept for alternative fuel operation [Volvo Group, 2007].

The approach based on igniting the port injected fuel using a small injection of fuel directly into the cylinder was pursued in this work. Ethanol was used as the premixed fuel, injected into the intake port, and was then ignited by injecting diesel into the cylinder. A major advantage compared to the work on pure port-fuel injection HCCI presented in the previous chapter is that no preheating is required for the ethanol to autoignite. The diesel fuel injection also provides an additional means of controlling combustion.

The direct-injected fuel could be expected to introduce stratification during the combustion process. A major point of interest is thus to study emissions and achievable operating range in this combustion mode. Ideally, a combustion process similar to that of HCCI operation is desired. Such operation requires that the majority of the fuel be mixed with air prior to combustion, meaning that rapid mixing of the diesel fuel with the ethanol-air charge is needed.

5.2 Control problem

The fumigation set-up used in this work has some similarities to dual-fuel HCCI operation. By increasing the ratio of fuel energy coming from diesel, combustion becomes faster. The fumigation set-up also presents additional features and complications. With the direct-injection diesel system, it is possible to modify not only the amount of diesel injected but also injection timing. With early injection, operation is closer to that of HCCI because the diesel fuel has time to partially mix with the ethanol-air mixture before combustion.

The set-up thus opens for the same difficulties in terms of controlling the combustion process as dual-fuel HCCI operation [Olsson *et al.*, 2001]. A too high diesel ratio would cause early ignition and thus high peak pressures and high pressure derivatives whereas a too low diesel ratio could result in incomplete combustion and high HC emissions.

Figure 5.1 shows in-cylinder pressure, cumulative heat released,

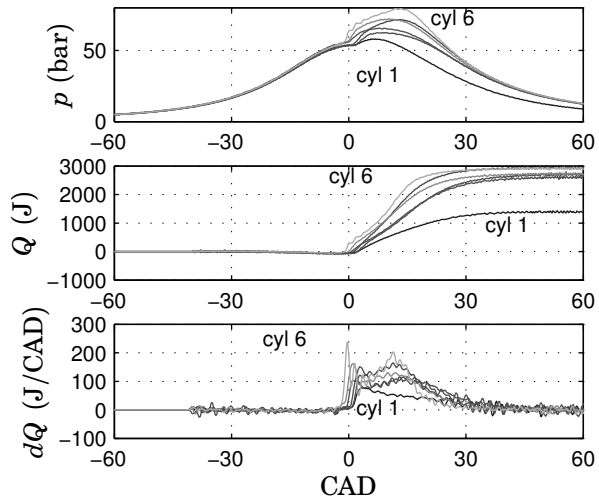

Figure 5.1 Pressure, cumulative heat released, and filtered heat release rate for six cylinders during a cycle at steady-state conditions.

and heat release rate for the six cylinders during one engine cycle. Nominal fuel injection parameters were the same for the six cylinders, i.e., the same signals were sent to the injector hardware. As can be seen, there is a large difference in the combustion process between the cylinders. It appears that for cylinder 1, the initial heat released from combustion of the diesel fuel is not sufficient to ignite the ethanol. On the other hand, for cylinder 6, heat release is very rapid, leading to high pressure derivatives.

There are many plausible causes for cylinder-to-cylinder differences in combustion, including:

- Fuel injectors do not inject equal amounts of fuel.
- Different compression ratios in cylinders due to geometrical variations.
- Volumetric efficiency varies due to variations in intake manifold fluid flow.

- Cooling water temperatures differ, resulting in different thermodynamic conditions for auto-ignition.

Cylinder-to-cylinder variations have been reported as an issue also in a previous fumigation study [Alger *et al.*, 2005], where EGR concentration variations were thought to be the main cause.

A major contributor to cylinder-to-cylinder variations in combustion is thought to be the diesel fuel injection system where unit injectors designed for conventional diesel operation were used. These injectors are calibrated for substantially larger diesel flows, so that the resolution is very poor at the levels used in the setting of this work. That implies that even though the injection duration was nominally the same for all cylinders, the injected amount may vary by a large factor among the cylinders.

It could be argued that if this combustion concept would be put in production, a diesel injection system adapted to the low diesel flows would be applied and the cylinder-to-cylinder variations would be reduced. Even so, there are other sources of cylinder-to-cylinder combustion variations that must be addressed, as noted in [Alger *et al.*, 2005].

The cylinder-to-cylinder variations severly limit the ability to perform the fumigation experiments, as well as the validity of the results. Parameters of interest, such as brake efficiency and emissions cannot be measured individually for each cylinder, and averaged values are of little interest when the combustion process differences are as large as in Figure 5.1. Moreover, too high peak cylinder pressures or high pressure derivatives in one cylinder would activate the safety mechanisms in the control system and shut down fuel injection. In short, in order to perform the experiments on fumigation, it is required to compensate for the variations.

5.3 Control structure

Closed-loop control was used to compensate for the cylinder-to-cylinder variations. The set-up can be seen as a form of automatic calibration that enables running the steady-state experiments.

In a research setting, this approach has several advantages. Elim-

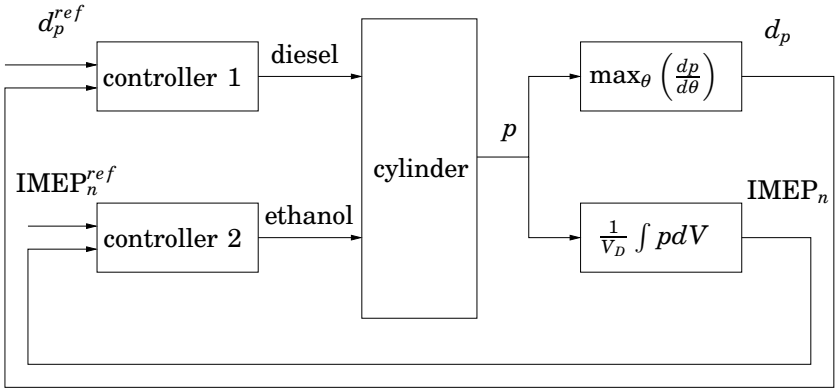

Figure 5.2 Control structure used for control of d_p and IMEP$_n$.

inating cylinder-to-cylinder variations results in well-defined operating conditions. Emissions and efficiency can be related to the actual combustion process observed in the pressure trace. Most importantly, differences in amount of fuel injected are automatically compensated for at each operating point, so that no extensive calibration of the fuel system is required.

To harmonize combustion between the cylinders, the amounts of the two fuels were manipulated. As feedback variables, the maximum pressure derivative during the cycle, d_p, and the net indicated mean effective pressure, IMEP$_n$, were used. It was found that if these variables were equal between the cylinders, pressure traces between the cylinders were similar.

Experimental testing showed that the maximum pressure derivative was strongly correlated with the amount of diesel injected. Therefore, the duration of diesel injection was used to control the pressure derivative to a setpoint, and the amount of ethanol injected was used to control IMEP$_n$ to a setpoint. The effect of varying the amount of diesel could be studied by varying the maximum pressure derivative setpoint. Both the d_p and the IMEP$_n$ controllers were of PI-type. The control structure is shown in Figure 5.2.

Controllers were designed ignoring the coupling between the two

control variables, diesel and ethanol injected, and the two measured variables, d_p and IMEP_n. Such couplings do exist, e.g. with a larger amount of diesel injected, IMEP_n will increase as the diesel fuel energy also contributes to the work output. To avoid exciting the cross-coupling, the controllers were tuned conservatively, which was satisfactory for the steady-state operation experiments presented here. For transient operation, a MIMO control design that takes into account the cross-coupled dynamics of the process should be developed.

5.4 Experimental conditions

Diesel was injected in the direct injection system, and ethanol in the port injection system. Inlet valve closing, u_{IVC}, was fixed at $u_{IVC} = 570$ throughout these experiments. The EGR rate and the VGT position were varied according to operating range, as described below. The engine speed was kept constant at 1450 rpm.

5.5 Results

Closed-loop versus open-loop operation

Figure 5.3 shows the spread in the two measured variables d_p and IMEP_n for 100 consecutive cycles with and without the controller activated. It can be seen that the cylinder-to-cylinder variations are significant in the latter case. Cylinders 1 and 6 with the lowest and highest IMEP_n, also demonstrate large cycle-to-cycle variations which are likely caused by incomplete combustion for cylinder 1, and large sensitivity of d_p for high loads for cylinder 6.

The controller completely eliminates the systematic cylinder-to-cylinder variations, and also reduces the cycle-to-cycle variations by placing all cylinders in an operating range where the combustion process is more stable.

The control set-up is thus very successful as a tool for automatic calibration in a laboratory setting. In practice, open-loop operation is preferred because it does not require sensors. An experiment was performed to see how well open-loop operation works once the diesel fuel

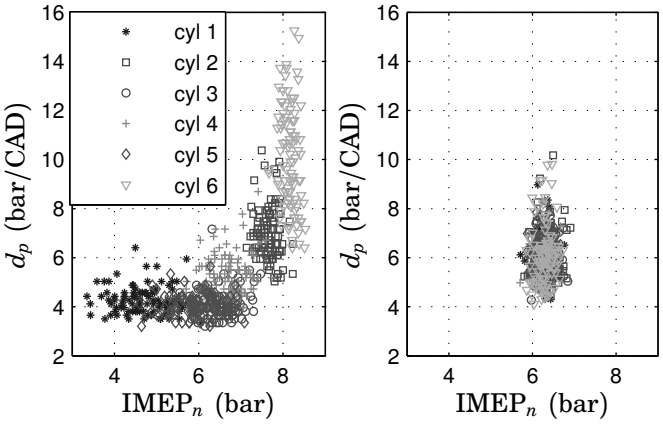

Figure 5.3 Maximum pressure derivative (d_p) and IMEP$_n$ for 100 consecutive cycles for the six cylinders, with all nominal conditions set equally (left), and with controller activated (right).

injection system has been calibrated. The controller was activated to find diesel injection parameters that maintained $d_p = 7$ bar/CAD at IMEP$_n = 8.5$ bar. These diesel injection settings were then frozen and the IMEP$_n$ was slowly increased to 11 bar by increasing the amount of ethanol. Figure 5.4 shows the resulting d_p for the six cylinders.

Two conclusions can be drawn from Figure 5.4. First, in order to keep d_p low, the amount of diesel must be carefully adjusted according to operating point. Second, settings for diesel injection duration that compensate for the cylinder-to-cylinder variations in the fuel injection system at one operating point are not immediately applicable at another operating point. Therefore, to enable operation in open loop, diesel parameters must be carefully mapped individually for each cylinder according to operating point. Open-loop operation is not impossible; there is very little dynamics from diesel injection duration to d_p, so there are no issues concerning instability necessitating closed-loop control. But to successfully operate the engine open-loop in a safe way, careful calibration based on either extensive experimental testing or accurate models of the combustion process is required.

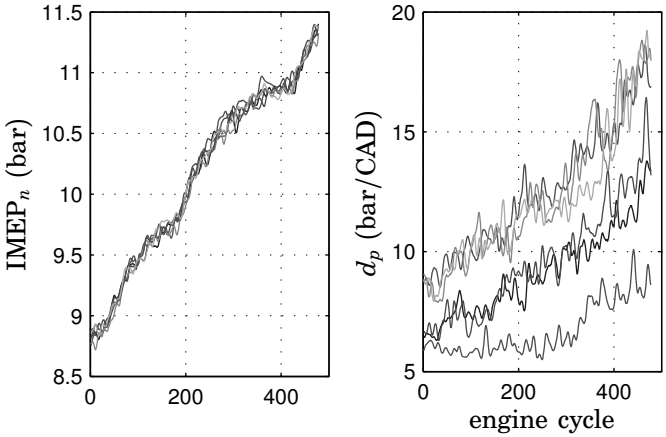

Figure 5.4 IMEP$_n$ and d_p during a load transient in open loop with fixed settings for diesel injection. The data are low-pass filtered to make trends more clearly visible.

Combustion process, efficiency, and emissions

Operation was tested at loads 4.6, 9.2, and 18.4 bar BMEP, corresponding to 25 %, 50 %, and 100 % of the maximum load specified for diesel operation of the engine.

Low load – 4.6 bar BMEP Four operation modes were tested:

1. Early fuel injection, 22° BTDC, with high EGR rate, 50%.
2. Early fuel injection, 22° BTDC, without EGR.
3. Late fuel injection, 7° BTDC, with high EGR rate, 45%.
4. Late fuel injection, 7° BTDC, without EGR.

For comparison purposes, the same operating point was also run with pure diesel operation without EGR.

For each of the operation modes, the ratio of fuel energy coming from diesel was varied by changing the setpoint for d_p. Figure 5.5 shows d_p setpoint versus diesel ratio for the four combustion modes.

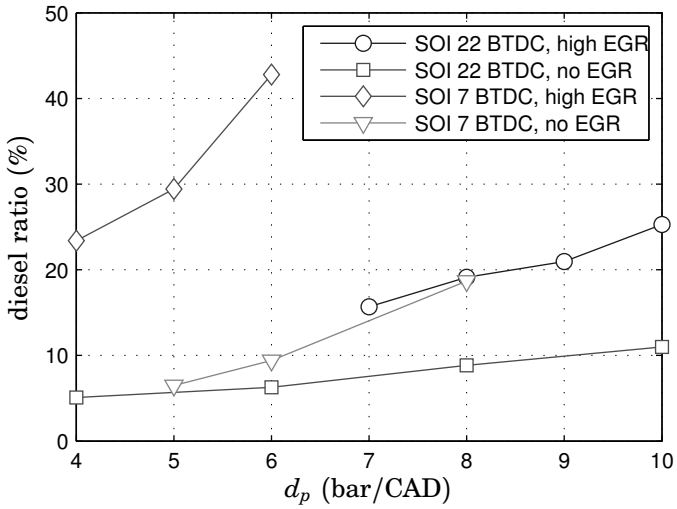

Figure 5.5 Ratio of diesel energy to total fuel energy required to keep a certain d_p for the four operation modes tested at 4.6 bar BMEP. With pure diesel operation without EGR, average d_p was 5.4 bar/CAD.

The range of d_p that was tested correspond to the range that was possible to obtain by modifying the diesel ratio without risk of misfire or too large cycle-to-cycle variations.

Heat release rates for the four combustion modes with different setpoints for d_p are shown in Figure 5.6. Heat release rates were computed from the cylinder pressure, and low-pass-filtered using a Hamming window of width $\pm$ 1 CAD.

A few things can be noted. First of all, cylinder-to-cylinder variations are small. The control structure, where d_p and IMEP$_n$ are harmonized between the cylinders, yields similar in-cylinder pressures and heat release rates in all cylinders. It can be concluded that d_p and IMEP$_n$ are suitable feedback variables.

With early diesel injection, a two-stage combustion was obtained. The magnitude of the first heat release peak was strongly correlated to the amount of diesel injection, cf. Figure 5.5. With a higher diesel

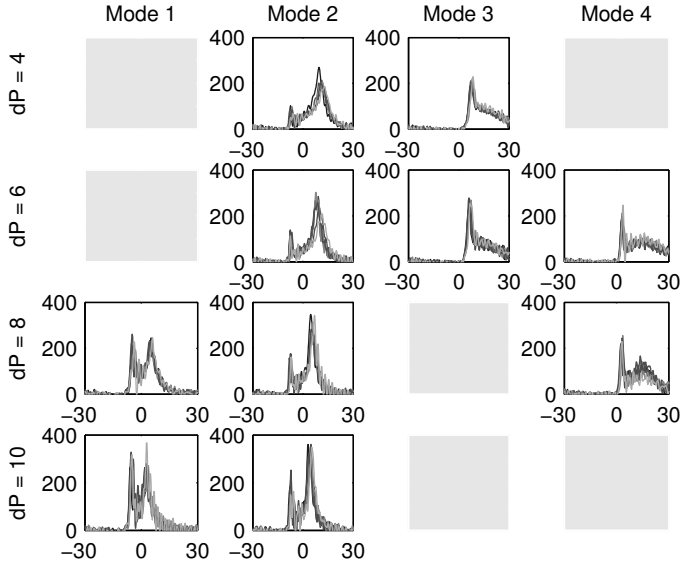

Figure 5.6 Experiments at 4.6 bar BMEP. Heat release rates (J/CAD) versus CAD for Mode 1–4 (left to right), for d_p = 4,6,8,10 (top to bottom).

ratio, the delay until the second heat release peak became shorter, and the heat release was faster. Without EGR, a smaller diesel ratio was required, and a larger part of the fuel is burned in the second heat release peak.

With late diesel injection, there was a single peak in the heat release rate. Heat release started shortly after TDC, then there was a short period of high heat release rate followed by a slowly decaying combustion rate.

Brake efficiencies and emissions are shown in Figure 5.7. HCCI-like levels of NO_x emissions were only obtained through late diesel injection and high EGR rate. In this combustion mode, CO emissions were very high and brake efficiency was low. Reasonably high efficiency, 33 % was obtained with early diesel injection and high EGR. In this combustion

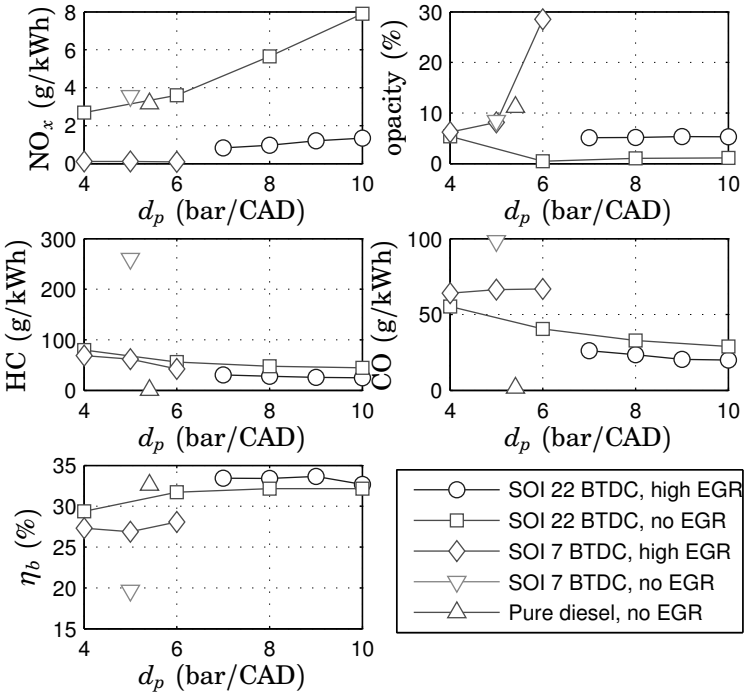

Figure 5.7 Emissions and brake efficiency for experiments at 4.6 bar BMEP.

mode soot was reduced compared to pure diesel operation, as was NO_x. However, NO_x was still in the order of 1 g/kWh and the maximum pressure derivatives were increased compared to the case of pure diesel operation.

Medium load – 9.2 bar BMEP Two operation modes were tested:

1. Early diesel injection, 22° BTDC, EGR = 45%.
2. Late diesel injection, 10° BTDC, EGR = 29%.

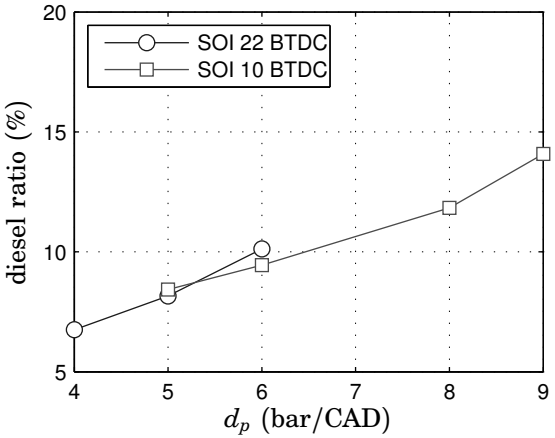

Figure 5.8 Diesel ratio required to keep a certain d_p for the two operation modes tested at 9.2 bar BMEP. With pure diesel operation, average d_p was 4.0 bar/CAD.

Operation without EGR was not possible due to risk of knock and too large cylinder-to-cylinder variations. Pure diesel operation was also tested for comparison purposes. Diesel ratio versus d_p is shown in Figure 5.8. With early diesel injection, the engine could be operated at a diesel ratio of 7–12 %, and with late diesel injection at a diesel ratio of 9–17 %.

Heat release rates for the two modes for different d_p setpoints are shown in Figure 5.9. With early diesel injection, there was a long ignition delay followed by a steadily increasing heat release rate. With late diesel injection, there was a two-stage combustion, with two peaks in the heat release.

Emissions and brake efficiencies are shown in Figure 5.10. Examining the emissions data, operation in Mode 1, with early diesel injection, shows interesting characteristics. Compared to pure diesel operation, NO_x emissions were reduced from the order of 3 g/kWh to the range 0.08 – 0.11 g/kWh. We can conclude that in this operation mode we obtain an HCCI-like combustion with low NO_x emissions. As is commonly

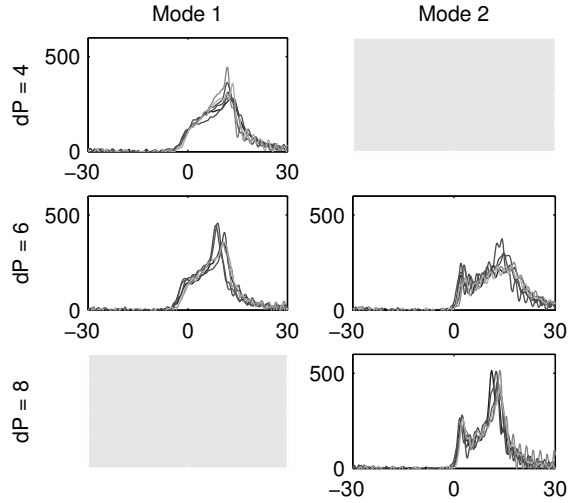

Figure 5.9 Experiments at 9.2 bar BMEP. Heat release rates (J/CAD) versus CAD for Mode 1–2 (left to right), for $d_p = 4,6,8$ (top to bottom).

observed in HCCI studies, HC and CO emissions were high, probably because of crevice effects and locally incomplete combustion.

High load – 18.4 bar BMEP Experiments were performed to find the high-load limit of fumigation operation. With closed-loop control, operation at 18.4 bar BMEP was possible with start of diesel injection at 9° BTDC. Data from this operating point is given in Table 5.1. Pressure curves and heat release rates from a cycle are shown in Figure 5.11.

Using the EGR system, the equivalent air fuel ratio λ was manually controlled to close to stoichiometric operation, which proved to give the most stable combustion at high load. Earlier diesel injection did result in lower NO_x, in analogy with the results at 9.2 bar BMEP, but also unstable combustion. Calibration around the 18.4 bar BMEP test point showed reasons to expect that even higher loads could have been achieved, had higher boost pressures been possible. With higher

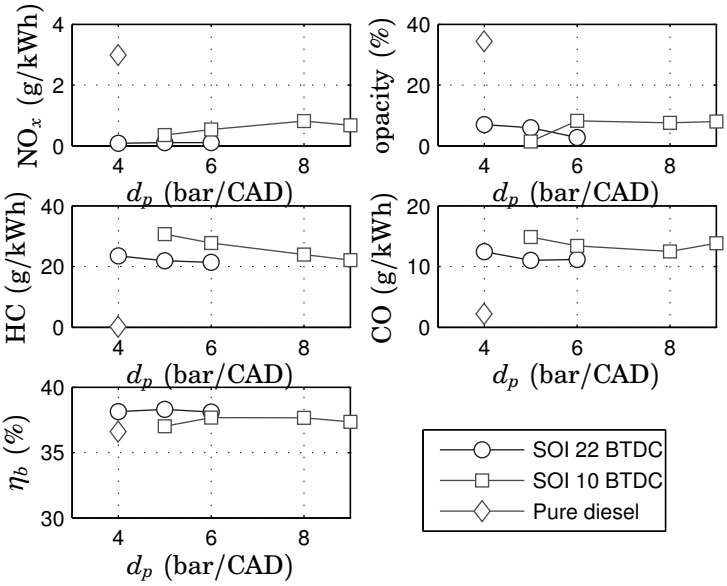

Figure 5.10 Emissions and brake efficiencies for experiments at 9.2 bar BMEP.

boost pressures, a higher EGR rate could have been used which could possibly reduce NO_x emissions at this load.

Pressure derivatives were modest, the reference for d_p was 5.5 bar/CAD. Figure 5.12 shows the distribution of d_p over 500 cycles. In most cycles, d_p is close to the reference. The frequency of cycles where d_p exceeded 15 bar/CAD was 0.53 %. The distribution of d_p is highly non-Gaussian, it appears that an exponential distribution could model the data well. The non-Gaussian character of the process noise needs to be taken into account in the control design if a faster controller that can handle transients is to be developed.

Table 5.1 Data from high load operation.

BMEP	18.4 bar
speed	1450 rpm
SOI	9° BTDC
intake pressure	2.25 bar
d_p	5.5 bar/CAD
diesel ratio	4.5 %
brake efficiency	38.0 %
NO_x	0.34 g/kWh
CO	33.7 g/kWh
HC	24.9 g/kWh
opacity	14%

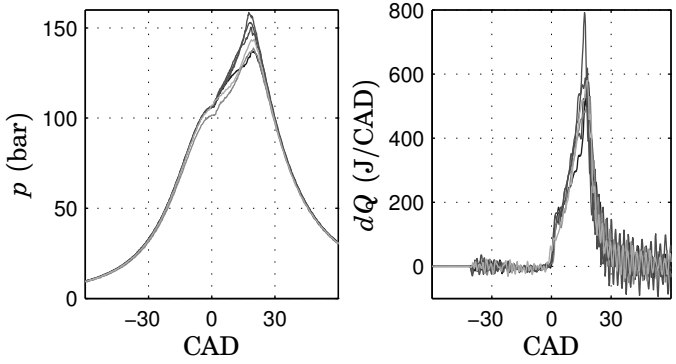

Figure 5.11 Pressure curves and heat release rates for operation at 18.4 bar BMEP.

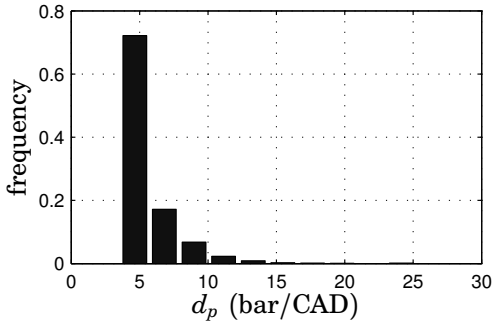

Figure 5.12 Distribution of d_p for operation at 18.4 bar BMEP.

6

Control of direct-injection diesel engine operation

6.1 Control objectives

For low-emission diesel engine operation, there is a clear trade-off between emissions of soot, NO_x, and brake efficiency as discussed in Chapter 2. To achieve target emissions levels, variable engine parameters must be carefully adjusted according to operating point since emissions are very sensitive, e.g. to EGR rate, see Figure 2.2. Actuator variables are typically injection timings, injection durations, injection pressures, number of injections, EGR and VGT valve positions, and possibly also VVA [Hafner *et al.*, 2000; Yilmaz and Stefanopoulou, 2003; Ortner and d. Re, 2007].

Much research has been presented on control of diesel engines with the objective of maximizing efficiency subject to constraints on emissions [Guzzella and Amstutz, 1998]. Depending on the type of low-emission diesel combustion that is desired, the control objective is different. For early-injection, high-EGR operation, there is a long ignition delay which results in conditions similar to that of port-fuel injection HCCI. Closed-loop control is necessary to stabilize the process or avoid drift from advantageous operating points due to disturbances such as varying air temperature. With less homogeneous conditions and shorter ignition delay, the purpose of control is rather to optimize

emissions trade-offs during transients [Hafner *et al.*, 2000; Ortner and d. Re, 2007].

In this work, EBP valve position u_{EGR} and start of injection angle u_{SOI} were chosen as control variables. The rationale for this choice was to use the conclusions from the many publications in the combustion engine literature relating EGR rate and injection timing to emissions, e.g., [Akihama *et al.*, 2001; Noehre *et al.*, 2006; Lewander *et al.*, 2008], to synthesize a closed-loop controller taking emissions into account during transients. To keep a reasonable efficiency, the engine was operated in a region with u_{EGR} corresponding to the left of the soot peak in Figure 2.2 where there is a clear NO_x-soot trade-off.

6.2 Control design

Actuators

Figure 6.1 shows steady-state data from [Lewander *et al.*, 2008] where NO_x, soot, brake efficiency, and the maximum pressure derivative d_p are mapped according to fuel injection timing u_{SOI} and EGR ratio r_{EGR} which is defined as the ratio of CO_2 concentration in the intake to the CO_2 concentration in the exhausts. It can be concluded from these maps that the four variables are sensitive to both u_{SOI} and u_{EGR} and with tight bounds on emissions, the allowed operating range becomes very narrow. The EGR ratio r_{EGR} is manipulated by the position of the EGR valve, u_{EGR}. It is difficult to accurately estimate r_{EGR} on-line during transient operation.

Running the engine in open-loop with low emissions will thus be a great challenge since emissions are very sensitive to the control variables, and even with extensive mapping small changes in the engine due to wear or natural production engine-to-engine differences could cause large deviations in emissions from the target values.

Feedback variables

For robust low-emission operation, it is desirable to use closed-loop control based on on-line measurements from the engine. Direct measurements of emissions are not possible, so some indirect measurements

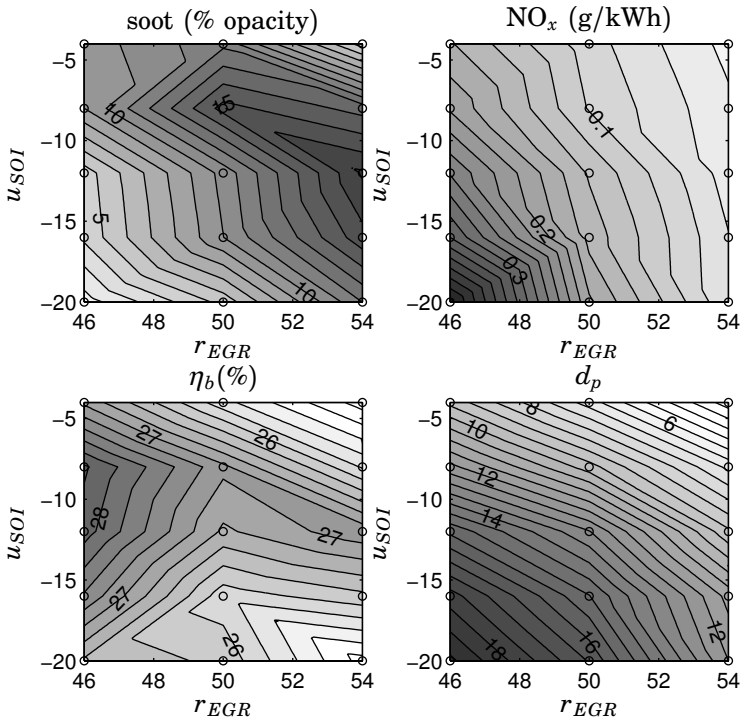

Figure 6.1 Emissions of NO$_x$ and soot, brake efficiency η_b, and pressure derivatives d_p mapped according to u_{SOI} and r_{EGR} in steady-state operation. Circles represent measurement points, intermediate values are obtained by linear interpolation.

that can predict emissions more robustly than the control variables alone are needed.

In Figure 6.2, the variables α_{50} and $\alpha_{ID} = \alpha_{10} - u_{SOI}$ are mapped according to u_{SOI} and r_{EGR}. These variables are sufficiently independent to be used as two independent feedback variables. From a physical point of view, one could also argue that these variables, the combustion phasing α_{50} and the ignition delay α_{ID} contain much information

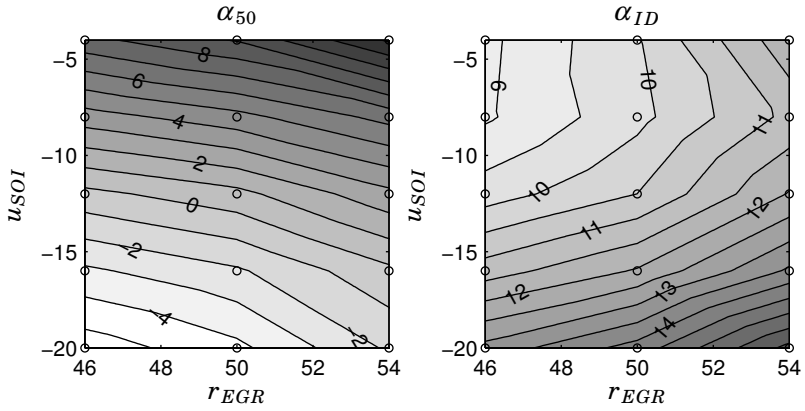

Figure 6.2 Feedback variables α_{50} and α_{ID} mapped according to u_{SOI} and r_{EGR} for steady-state operation.

about the actual combustion process and should therefore be suitable for prediction of emissions. A physical model relating emissions of NO_x and soot to α_{50} and α_{ID} would be highly desirable, but in this work empirical data are used to relate emissions to the measured variables.

Figure 6.3 shows emissions mapped according to α_{50} and α_{ID}. Note that these data were collected at a different load than the data in Figure 6.1. The levels of emissions are therefore different, but the NO_x-soot trade-off shows the same characteristics. Figure 6.4 shows a weighted sum of NO_x and soot which defines a cost function to be minimized. Also plotted in Figure 6.4 are level contours of a quadratic cost function that approximates the emissions cost and which will form the basis for the LQG controller.

Problem formulation

Let the dynamics of cylinder i, $i \in \{1,\dots 6\}$, from input u^i_{SOI} and u_{EGR} to output $y^i = (\alpha^i_{50} \quad \alpha^i_{ID})^T$ be modelled by a linear time-invariant

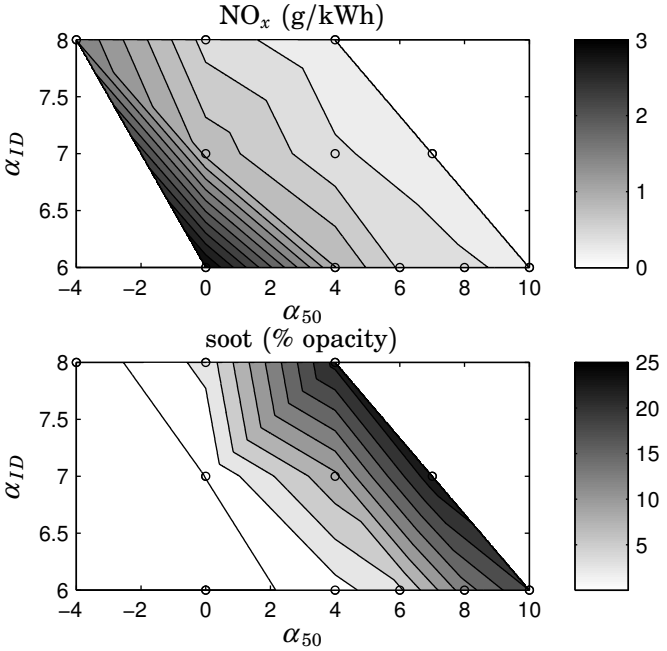

Figure 6.3 Emissions of NO_x and soot mapped according to α_{50} and α_{ID} in steady-state operation. Circles represent measurement points, intermediate values are obtained by linear interpolation.

discrete-time system

$$\begin{aligned} x^i_{k+1} &= A^i x^i_k + \begin{pmatrix} B^i_1 & B^i_2 \end{pmatrix} \begin{pmatrix} u^i_{SOI,k} \\ u_{EGR,k} \end{pmatrix} + K^i w^i_k \\ y^i_k &= C^i x^i_k + \begin{pmatrix} D^i_1 & D^i_2 \end{pmatrix} \begin{pmatrix} u^i_{SOI,k} \\ u_{EGR,k} \end{pmatrix} + w^i_k \end{aligned} \tag{6.1}$$

where the input u_{SOI} can be set individually for each cylinder whereas u_{EGR} is a common control variable influencing all cylinders. Let n denote the system order, then $u^i_{SOI} \in \mathbb{R}$, $u_{EGR} \in \mathbb{R}$, $y^i \in \mathbb{R}^2$, $x^i \in \mathbb{R}^n$,

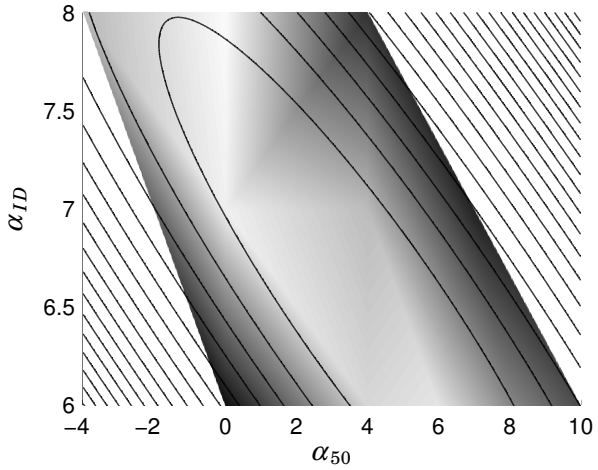

Figure 6.4 Weighted sum of emissions from Figure 6.3 and level contours of cost function to be minimized.

and $w^i \in \mathbb{R}^2$. The sample time is one engine cycle. The noise w_k is zero-mean white Gaussian noise with

$$\mathrm{E}(w_k^i w_k^{iT}) = Q_n^i.$$

The objective of the controller is to minimize the quadratic cost function

$$J(u^i) = \lim_{k\to\infty} \mathrm{E}\left(\sum_{i=1}^{6}(r_k^i - y_k^i)^T Q^i (r_k^i - y_k^i) + I_k^{iT} Q_I^i I_k^i + u_k^{iT} R^i u_k^i\right) \quad (6.2)$$

where I_k^i represents integrator states, the matrices Q^i define the level contours in Figure 6.4, and the weight matrices Q_I^i and R^i represent cost on the integrator states and control variables. The reference value r_k is assumed to be constant.

The dynamics of the full six-cylinder engine can now be written as

$$\begin{aligned} x_{k+1} &= Ax_k + Bu_k + Kw_k \\ y_k &= Cx_k + Du_k + w_k \end{aligned} \quad (6.3)$$

where

$$
\begin{aligned}
A &= \mathrm{diag}\{A^1, \cdots, A^6\} \\
B &= \begin{pmatrix} B_1^1 & 0 & \cdots & 0 & B_2^1 \\ 0 & B_1^2 & \cdots & 0 & B_2^2 \\ \vdots & \vdots & \ddots & \vdots & \vdots \\ 0 & \dots & \cdots & B_1^6 & B_2^6 \end{pmatrix} \\
K &= \mathrm{diag}\{K^1, \cdots, K^6\} \\
C &= \mathrm{diag}\{C^1, \cdots, C^6\} \\
D &= \begin{pmatrix} D_1^1 & 0 & \cdots & 0 & D_2^1 \\ 0 & D_1^2 & \cdots & 0 & D_1^2 \\ \vdots & \vdots & \ddots & \vdots & \vdots \\ 0 & \dots & \cdots & D_1^6 & D_2^6 \end{pmatrix}
\end{aligned}
$$

and

$$
\begin{aligned}
x &= \begin{pmatrix} x_1^T & \cdots & x_6^T \end{pmatrix}^T, & x &\in \mathbb{R}^{6n} \\
u &= \begin{pmatrix} u_{SOI}^1 & \cdots & u_{SOI}^6 & u_{EGR} \end{pmatrix}^T, & u &\in \mathbb{R}^7 \\
y &= \begin{pmatrix} y_1^T & \cdots & y_6^T \end{pmatrix}^T, & y &\in \mathbb{R}^{12} \\
\mathrm{E}(w_k w_k^T) &= Q_n = \mathrm{diag}\{Q_n^1, \cdots, Q_n^6\}.
\end{aligned}
$$

The optimization problem (6.2) can now be reformulated as

$$
J(\{u_k\}) = \min_{\{u_k\}} \lim_{k\to\infty} \mathrm{E}\left((r_k - y_k)^T Q (r_k - y_k) + I_k^T Q_I I_k + u_k^T R u_k \right) \quad (6.4)
$$

where $\{u_k\}$ is a causal function of $\{y_k\}$,

$$
\begin{aligned}
Q &= \mathrm{diag}\{Q^1, \cdots, Q^6\} \\
Q_I &= \mathrm{diag}\{Q_I^1, \cdots, Q_I^6\}
\end{aligned}
$$

and R represents the cost of the seven control variables.

Centralized LQG

A controller for the 7-input, 12-output system (6.3) that minimizes the cost (6.4) can be designed using standard LQG techniques [Åström and

Wittenmark, 1997] by extending the state vector with the integrator states according to

$$z_k = \begin{pmatrix} x_k \\ I_k \end{pmatrix}. \tag{6.5}$$

The standard integrator update equation is

$$I_{k+1} = I_k + r_k - y_k$$

but for the system (6.3) with $u_k \in \mathbb{R}^7$ and $y_k \in \mathbb{R}^{12}$, the extended system will not be stabilizable, and the optimization problem (6.4) will not be well posed because $\mathrm{E}(I_k^T Q_I I_k)$ will not be finite for any control law $u_k = -L_C z_k$.

To find a modified integrator update equation, consider the extended system using the standard integrator update (6.5),

$$\begin{pmatrix} x_{k+1} \\ I_{k+1} \end{pmatrix} = \begin{pmatrix} A & 0 \\ -C & I \end{pmatrix} \begin{pmatrix} x_k \\ I_k \end{pmatrix} + \begin{pmatrix} B \\ -D \end{pmatrix} u_k + \begin{pmatrix} 0 \\ I \end{pmatrix} r_k + \begin{pmatrix} K \\ -I \end{pmatrix} w_k.$$

Denote by W_c the controllability matrix for this system. The non-controllable part of I_k is given by

$$W_C^T \begin{pmatrix} x_k \\ I_k \end{pmatrix} = 0$$
$$\begin{pmatrix} I & 0 \end{pmatrix} \begin{pmatrix} x_k \\ I_k \end{pmatrix} = 0$$

which can be written as

$$\begin{pmatrix} W_C^T \\ I \quad 0 \end{pmatrix} \begin{pmatrix} x_k \\ I_k \end{pmatrix} = \begin{pmatrix} N_x & N_I \end{pmatrix} \begin{pmatrix} x_k \\ I_k \end{pmatrix} = 0$$

where N_x and N_I are matrices of appropriate dimensions.

We wish to find a projection matrix M such that

$$\bar{I}_k = M I_k,$$

where $\mathrm{rank}(M) = \mathrm{rank}(N_I)$, and $\bar{I}_k$ represents the controllable part of I_k.

The matrix M should then satisfy $N_I = N_I M$ and $\text{rank}(M) = \text{rank}(N_I) = 7$ since there are seven independent inputs to the system. From the singular value decomposition of N_I, it holds that

$$\begin{aligned} N_I &= U\Sigma V^T = U\Sigma \begin{pmatrix} I_{7\times 7} & 0 \\ 0 & 0_{5\times 5} \end{pmatrix} V^T \\ &= \underbrace{U\Sigma V^T}_{N_I} \underbrace{V \begin{pmatrix} I_{7\times 7} & 0 \\ 0 & 0_{5\times 5} \end{pmatrix} V^T}_{M} = N_I M. \end{aligned}$$

Now define the integrator update equation as

$$I_{k+1} = M(I_k + r_k - y_k) \tag{6.6}$$

which will only update I_k along its controllable modes, in practice yielding seven independent integrators for the seven-input system (6.3).

LQG controllers can now be designed for the extended system

$$\begin{aligned} z_{k+1} &= \begin{pmatrix} A & 0 \\ -MC & M \end{pmatrix} z_k + \begin{pmatrix} B \\ -MD \end{pmatrix} u_k + \begin{pmatrix} 0 \\ M \end{pmatrix} r_k + \begin{pmatrix} K \\ -M \end{pmatrix} w_k \\ y_k &= \begin{pmatrix} C & 0 \end{pmatrix} z_k + Du_k + w_k. \end{aligned} \tag{6.7}$$

The Kalman filter for state observation is given by

$$\hat{x}_{k+1} = A\hat{x}_k + L_F(y_k - C\hat{x}_k - Du_k)$$

and the optimal control law by $u_k = -L_C \begin{pmatrix} \hat{x}_k^T & I_k^T \end{pmatrix}^T + L_R r_k$. The gains L_F and L_C are found by solving the Riccati equations, as described in [Åström and Wittenmark, 1997]. The optimal reference value weight matrix L_R is computed using the procedure in [Haddad and Moser, 1994].

Decentralized LQG

A disadvantage with the controller presented in the previous section is that measurements from all cylinders must be available to compute any single control variable. The resulting controller is designed for a

seven-input, twelve-output system and with an n-state model for each cylinder, the extended system (6.7) will be of order $n_e = 6n + 12$.

An alternative approach is suggested here where the control laws for u^i_{SOI} are based on local measurements of y^i only. The approach relies on the following assumptions

1. all cylinders have identical dynamics
2. the controller for u_{EGR} should be slower than u_{SOI}.

Both assumptions are reasonable; it has been shown that identified dynamical models for the six cylinders differ in terms of offsets but the differences in dynamics are negligible, and u_{EGR}, which is the position of a valve, will have some inherent inertia that makes very fast changes infeasible whereas it is possible to change injection timings freely from one engine cycle to the next.

The decentralized approach relies on designing the controllers for u_{SOI} and u_{EGR} separately. First, u_{EGR} is considered as a constant, measurable disturbance, and an LQG controller for u_{SOI} is designed for the single cylinder system (6.1) extended with integrator states

$$\begin{aligned}
\begin{pmatrix} x^i_{k+1} \\ I^i_{SOI,k+1} \end{pmatrix} &= \begin{pmatrix} A^i & 0 \\ -M^i_{SOI}C^i & M^i_{SOI} \end{pmatrix} \begin{pmatrix} x^i_k \\ I^i_{SOI,k} \end{pmatrix} \\
&+ \begin{pmatrix} B^i_1 \\ -M^i_{SOI}D^i_1 \end{pmatrix} u^i_{SOI,k} + \begin{pmatrix} B^i_2 \\ -M^i_{SOI}D^i_2 \end{pmatrix} u_{EGR,k} \\
&+ \begin{pmatrix} 0 \\ M^i_{SOI} \end{pmatrix} r_k + \begin{pmatrix} K^i \\ -M_{SOI} \end{pmatrix} w_k \\
y_k &= \begin{pmatrix} C^i & 0 \end{pmatrix} \begin{pmatrix} x^i_k \\ I^i_{SOI,k} \end{pmatrix} + D^i_1 u^i_{SOI,k} + D^i_2 u_{EGR,k} + w_k.
\end{aligned} \tag{6.8}$$

The integrator update projection matrices M^i_{SOI} are chosen such that the integrator states are only updated in directions controllable by u^i_{SOI}, analogously to the procedure described in the previous section.

Standard Kalman filters are used to estimate $\hat{x}^i$, and controllers

$$u^i_{SOI,k} = -L^i_{C,SOI} \begin{pmatrix} \hat{x}^i_k \\ I^i_{SOI,k} \end{pmatrix} + L^i_V u_{EGR,k} + L^i_{R,SOI} r_k \tag{6.9}$$

are designed that minimize the term of the cost function (6.2) for each cylinder over $\{u^i_{SOI}\}$ where $\{u^i_{SOI}\}$ are causal functions of $\{y^i\}$, r, and u_{EGR}. The control law for u^i_{SOI} depends on measurements y^i only, and the system dynamics (6.8) is of order $n_{ecyl} = n + 2$, six times less than the order of (6.7).

To design a controller for u_{EGR}, consider the closed-loop system obtained by inserting the control law (6.9) into the dynamics (6.8). Design an LQG controller that minimizes the cylinder cost function

$$J(u_{EGR}) = \lim_{k\to\infty} \mathrm{E}((r^i_k - y^i_k)^T Q^i (r^i_k - y^i_k) + I^{iT}_{SOI,k} Q_I I_{SOI,k} + I^{iT}_{EGR,k} Q_{I2} I^i_{EGR,k} + R_{EGR} u^2_{EGR,k})$$

subject to the dynamics given by (6.8) and (6.9) extended by integrator states I_{EGR} that are updated along directions controllable by u_{EGR}.

For cylinder i, the resulting optimal control law will then take the form

$$u^i_{EGR,k} = -L^i_{C,EGR} \begin{pmatrix} \hat{x}^i_k \\ I^i_{SOI,k} \\ I^i_{EGR,k} \end{pmatrix} + L^i_{R,EGR} r_k$$

where the optimal $u^i_{EGR,k}$ will vary between the cylinders. With identical dynamics for all cylinders, $L^i_{C,EGR} = L_{C,EGR}$ and $L^i_{R,EGR} = L_{R,EGR}$ are the same for all cylinders. Choose u_{EGR} as the average optimal u^i_{EGR}

$$u_{EGR,k} = -L_{C,EGR} \begin{pmatrix} \frac{1}{6}\sum_{i=1}^6 \hat{x}^i_k \\ \frac{1}{6}\sum_{i=1}^6 I^i_{SOI,k} \\ I_{EGR,k} \end{pmatrix} + L_{R,EGR} r_k$$

and update I_{EGR} according to

$$I_{EGR,k+1} = M_{EGR} \left(I_{EGR,k} + r_k - \frac{1}{6} \sum_{i=1}^6 y^i_k \right).$$

6.3 Modelling

System identification [Johansson, 1993] from experimental process data was used to identify dynamic models of the form (6.1). Data were col-

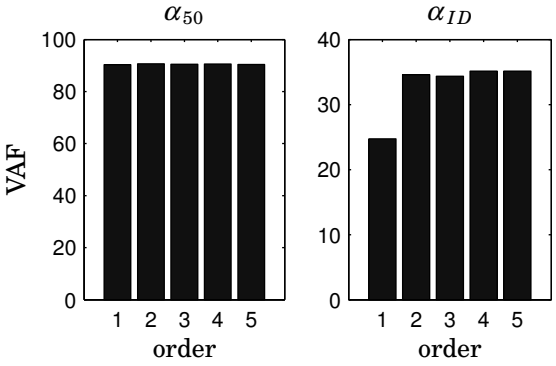

Figure 6.5 Variance accounted for models of different orders for one of the cylinders.

lected in open loop where the system was excited with PRBS (pseudo-random binary sequence) signals for the two inputs. Data sets of length 900 engine cycles were used for identification and validation respectively. Identification of state-space models was performed using the Matlab System Identification Toolbox command `pem` which uses a combination of subspace identification and minimization of prediction error.

Figure 6.5 shows variance accounted for (VAF), for models of order $n = 1$ to $n = 5$ for one cylinder. VAF is defined as

$$VAF = 100 \left(1 - \frac{\text{var}(y - \hat{y})}{\text{var}(y)} \right).$$

Prediction of α_{50} is as good with a first order model as for models of higher orders, but prediction of α_{ID} becomes significantly better using a second-order model. Second-order models were therefore used for control design.

It can be seen that a larger portion of the variance in α_{50} is captured by the model than the variance in α_{ID}. This effect is caused by larger excitation from u_{SOI} and u_{EGR} to α_{50}.

Models estimated from identification data from the six cylinders are simulated against validation data from all cylinders, and VAF for

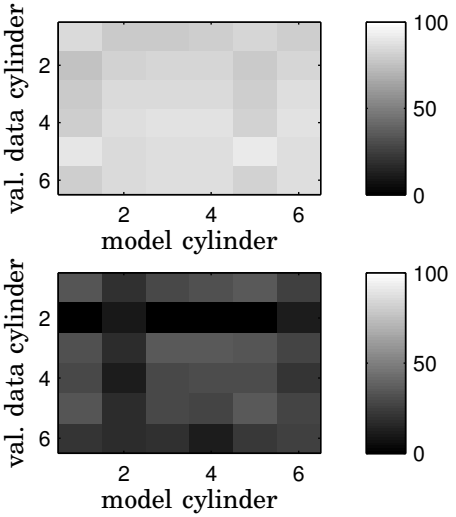

Figure 6.6 Variance accounted for (VAF) for α_{50} (top), and α_{ID} (bottom), for validation data for the six cylinders matched to models estimated from identification data for the six cylinders.

all combinations are shown in Figure 6.6. There is no clear trend that models from the same cylinder better predict data than models estimated from different cylinders, which would have been indicated by higher VAF values on the diagonals in the figure. It thus seems reasonable to use the same model for all cylinders in the control design.

Figure 6.7 shows validation data and predicted output for one cylinder with a second-order model. The idenfication was performed on data with the same input amplitudes and parameters for generation of the PRBS sequence.

6.4 Experimental conditions

All engine variables except u_{SOI} and u_{EGR} were kept constant. The experiments were performed at a constant fuel injection duration of

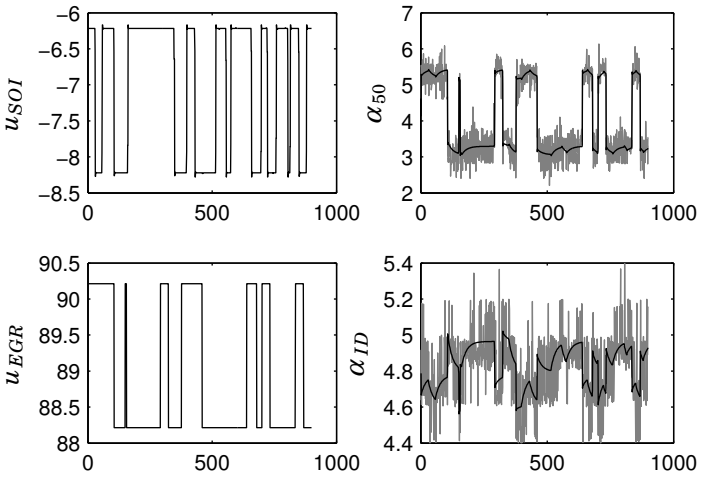

Figure 6.7 Cross validation of identified model for one cylinder with data not used for identification. The plots to the right show measured outputs (gray), and predicted output (black).

7 CAD, corresponding to $\text{IMEP}_n = 5.8$ bar, and at engine speed $N = 1200$ rpm. Inlet valve closing angle was kept constant at $u_{IVC} = 560$. The VGT valve was also kept constant, giving an absolute inlet pressure of $p_{in} = 1.12$ bar.

6.5 Results

The controllers were tested both in simulation and experiment. All model parameters including the noise characteristics were taken from the identified model. The costs for the outputs, $Q^i = Q^0$, were defined by the level contours demonstrated in Figure 6.4 giving identical costs for all cylinders, and the integrator costs were chosen as $Q_I^i = \gamma Q^0$, $Q_{I2}^i = \gamma_2 Q^0$. The control variable cost R was adjusted to keep the cycle-to-cycle changes in the control variables within realistic bounds. The

reference value for y_k, i.e., the center point in Figure 6.4, is shifted in the results presented because the optimal point varies somewhat with operating conditions such as speed and fuel injection pressure.

In all presented results, the reference value is first set different from the cost function optimum, and then shifted to the optimum after a few cycles. This way, we can observe the transient performance of the closed-loop system after a disturbance has shifted the system from its setpoint.

Simulations

Results from a Simulink simulation of the engine with the centralized LQG controller are shown in Figure 6.8.

From this figure, it can be seen that there is a large overshoot in α_{50} when the reference value is changed. In Figure 6.9 the process output y_k is shown in relation to the cost function level contours. Here, it can be seen that the overshoot in α_{50} occurs in a direction of decreasing cost, and that the cost demonstrates a monotonic convergence to its stationary value. The reason why this convergence does not happen in the shortest geometrical path from the initial to the final reference value is the combined effect of the skewed cost function level contours, the cost on the control signals, and the system dynamics, i.e., because of the slow changes of u_{EGR} and the slower effect on α_{ID} compared to α_{50}.

It can be concluded from Figure 6.9 that the cylinder-to-cylinder differences are quite small, so that the performance is not in practice limited by the configuration where $y \in \mathbb{R}^{12}$ and $u \in \mathbb{R}^7$.

Simulation results using the decentralized controller are shown in Figures 6.10 and 6.11. Performance is similar to the centralized controller, and the differences are primarily caused by different weighting matrices in the cost function.

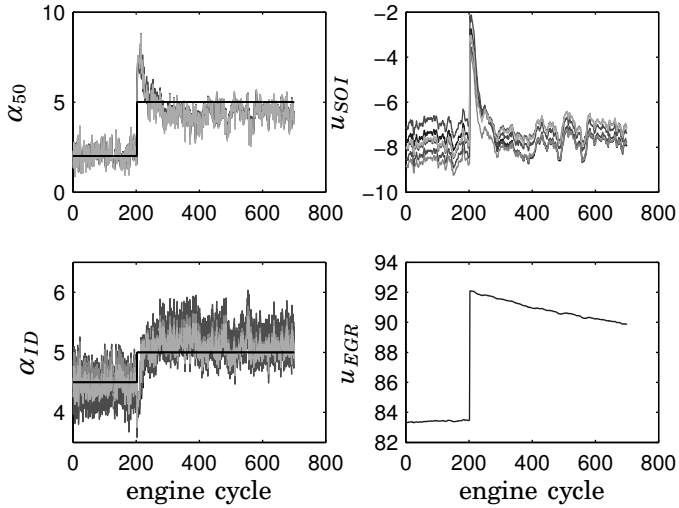

Figure 6.8 Simulation results using the centralized controller. At engine cycle 100, the reference value is changed to the cost function optimum.

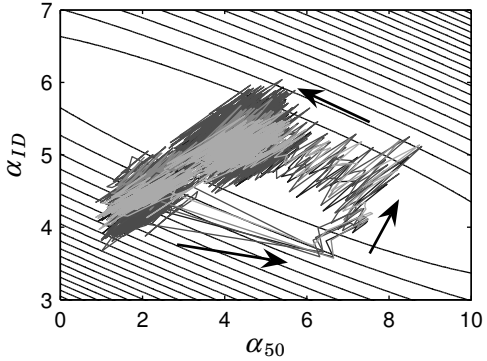

Figure 6.9 Simulation results using the centralized controller from Figure 6.8. The outputs y_k are shown together with level contours for the cost function. The reference value is first $(\alpha_{50}^{ref}, \alpha_{ID}^{ref}) = (2, 4.5)$ and then at engine cycle 200 changed to the cost function optimum at $(\alpha_{50}^{ref}, \alpha_{ID}^{ref}) = (5, 5)$. The arrows indicate the direction of the trajectories.

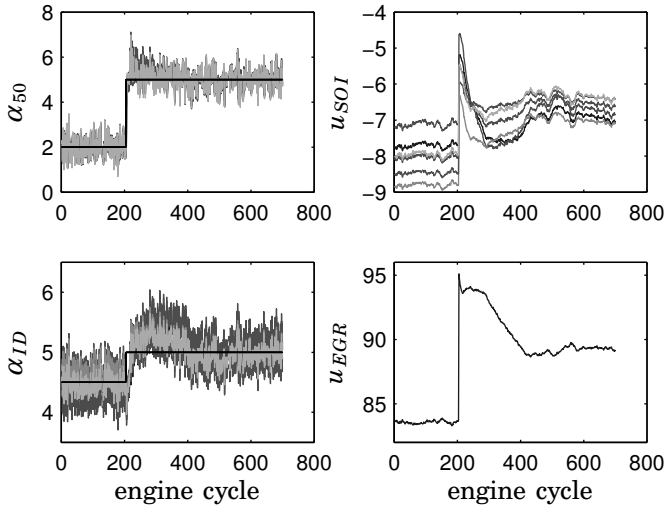

Figure 6.10 Simulation results using the decentralized controller. At engine cycle 100, the reference value is changed to the cost function optimum.

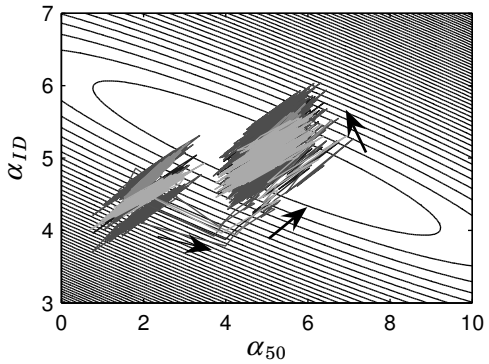

Figure 6.11 Simulation results using the decentralized controller from Figure 6.10. The outputs y_k are shown together with level contours for the cost function.The reference is changed from $(\alpha_{50}^{ref}, \alpha_{ID}^{ref}) = (2, 4.5)$ to $(\alpha_{50}^{ref}, \alpha_{ID}^{ref}) = (5, 5)$ at engine cycle 200. The arrows indicate the direction of the trajectories.

Experiments

Experimental results using the centralized controller are shown in Figures 6.12 and 6.13. Performance is similar to what was seen in simulations. The control variable u_{EGR} saturates at its upper value when the reference is changed. An anti-windup feature would be desirable but has not been implemented here, nevertheless the control variable gets out of the saturation rapidly and the effect of the saturation on control performance appears to be limited. Though there are large overshoots in the step response transients in Figure 6.12, it can be seen in Figure 6.13 that the transient takes place in a direction associated with low cost.

Experimental results using the decentralized controller are shown in Figures 6.14 and 6.15. It is less clear that the cost function is minimized subject to the control variable cost in this case, and the decentralized controller was more difficult to tune compared to the centralized controller. The reason is thought to be the two-stage design method, where the effect of changing one weighting matrix is less transparent than for the one-stage design method used for the centralized controller.

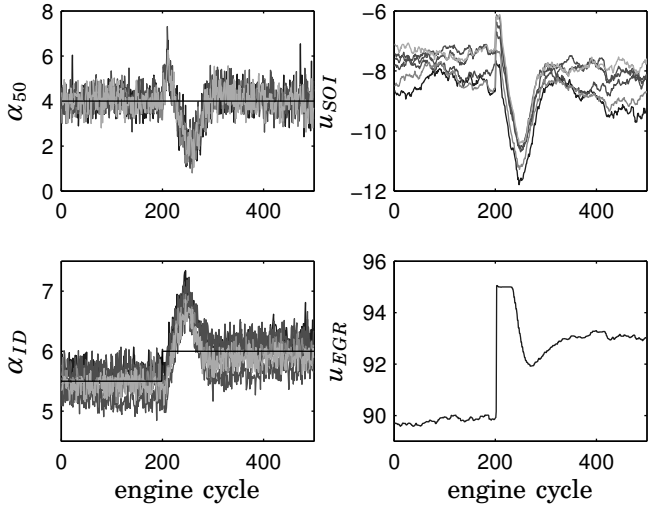

Figure 6.12 Experimental results using the centralized controller. At engine cycle 200, the reference value is changed to the cost function optimum.

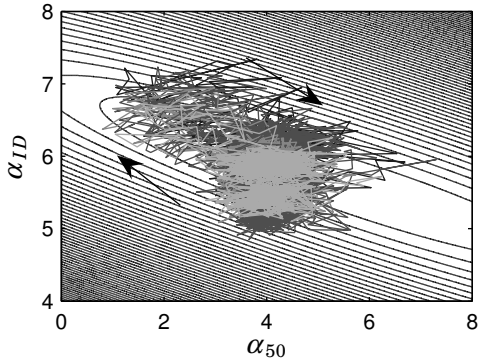

Figure 6.13 Experimental results using the centralized controller from Figure 6.12. The outputs y_k are shown together with level contours for the cost function. At engine cycle 200, the reference is changed from $(\alpha_{50}^{ref}, \alpha_{ID}^{ref}) = (4, 5.5)$ to $(\alpha_{50}^{ref}, \alpha_{ID}^{ref}) = (4, 6)$. The arrows indicate the direction of the trajectories.

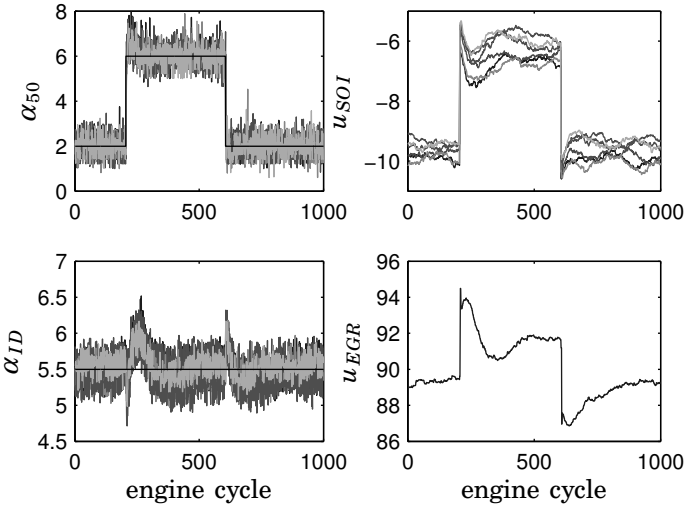

Figure 6.14 Experimental results using the decentralized controller. At engine cycle 200, the reference value is changed to the cost function optimum. At engine cycle 600, the reference value is changed back to the original value. From the different responses on the positive and negative reference step, it can be concluded that the process is nonlinear even for small changes in reference value.

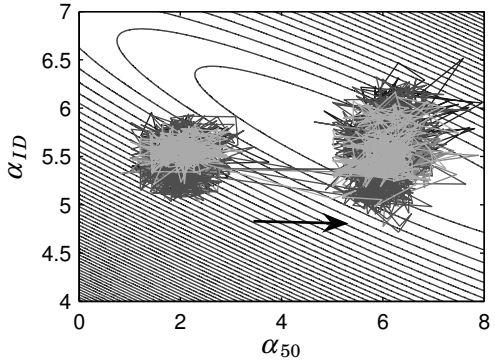

Figure 6.15 Experimental results using the decentralized controller. The outputs y_k are shown together with level contours for the cost function for data for engine cycle 1 to 500 in Figure 6.14. At engine cycle 200, the reference value is changed from $(\alpha_{50}^{ref}, \alpha_{ID}^{ref}) = (2, 5.5)$ to the cost function optimum at $(\alpha_{50}^{ref}, \alpha_{ID}^{ref}) = (6, 5.5)$. The arrow indicates the direction of the trajectory.

7

Conclusions and future work

7.1 Conclusions

Low-emission engine concepts are promising as alternatives or complements to advanced after-treatment systems when it comes to reducing pollutant emissions from heavy-duty engines. To adapt the combustion conditions so that low levels of emissions are achieved over a large operating range, such engines typically have added degrees of freedom in terms of new actuators. In order to make the engine set-up cost-effective, each new degree of freedom added to the engine must be optimally used, and here control plays an important role.

In this thesis, benefits of closed-loop control have been shown for three different engine configurations. However, the purpose of the control system was quite different in the three cases, as were the control structures. To communicate the benefits of closed-loop control, it is important to pinpoint the objective of control and to state the advantages. This chapter provides a summary of the presented results, and attempts to motivate how the proposed solutions could be integrated into complete engine control systems.

Control of port-fuel injection engine operation

Purpose Compression ignition of a homogeneous mixture created in the intake manifold is inherently very sensitive to operating conditions such as engine speed, load, and temperature. To maintain a favorable combustion phasing, it is thus imperative to adjust some actuator variable to counteract these load disturbances. Because wall heat transfer effects create cycle-to-cycle interactions in combustion phasing which at higher loads can become unstable, closed-loop control is necessary to operate the engine.

The purpose of the work on the mid-ranging control structure was to maintain good load disturbance rejection and stabilization of the process over a larger operating range than what is possible with only one actuator. Operating range extension is a key issue in making the HCCI engine feasible for production. Thus, it is of interest to study control structures that combine two or more actuator variables to control the combustion phasing over a larger operating range.

Benefits of control The experimental results verifed that the problem with a limited operating range of u_{IVC} can be successfully remedied by varying the EGR rate. It was shown that the mid-ranging control structure is very well suited for the combustion phasing control problem by combining the fast, cylinder-individual actuation of the VVA system with the slower and less accurate actuation obtained with variable EGR.

The control structure is intuitive and simple to implement. Since it changes u_{EGR} continuously to reset u_{IVC} to its reference, there is no need for extensive engine maps which require extensive testing. If linear controllers are used, as in the experimental work presented here, the closed-loop system is simple to analyze as compared to *ad hoc* solutions where u_{EGR} is changed according to some heuristic logic.

The results could easily be generalized to other actuator combinations, as long as at least one of the actuators is cylinder-individual and capable of cycle-to-cycle actuation.

In the HCCI operating range, the mid-ranging controller can be used to maintain a favorable combustion phasing. A higher-level control loop should determine the reference value for the combustion phasing taking into account efficiency, emissions, and audible noise.

Control of fumigation operation

Purpose Cylinder-to-cylinder variations pose a significant problem when operating a multi-cylinder engine. The origin of the variations may be systematic, such as heat transfer characteristics that will not vary from engine to engine, or random, such as injectors with low accuracy. To draw conclusions from multi-cylinder experiments, the cylinder-to-cylinder variations should be kept at a minimum.

In production engines, systematic cylinder-to-cylinder variations could be eliminated by modeling the causes and compensating for them. Random cylinder-to-cylinder variations could be reduced by reducing the tolerances in the instrumentation.

In a laboratory setting, it is desirable to avoid spending a large effort on modeling and compensating for effects that are not directly part of the study at hand, and one normally wants to make do with the available actuators. On the other hand, in a laboratory setting, there is normally both sensors and computing resources available which could be used for closed-loop control.

In the fumigation experiments presented here, poor accuracy of the injectors in the investigated fuel injection duration range resulted in very large cylinder-to-cylinder variations that made it difficult to operate the engine, and to draw any conclusions from the results. Closed-loop control was used for automatic calibration at each operating point, thus eliminating the need for exhaustive mapping efforts.

Benefits of control The control structure, with closed-loop control of IMEP_n and d_p proved successful in eliminating the cylinder-to-cylinder variations in steady state. By positioning all cylinders in a favorable region of the IMEP_n-d_p plane, the cycle-to-cycle variations were also reduced compared to open-loop operation. The resulting stable combustion process enabled running experiments at medium and high load that would not have been possible in open-loop without exhaustive calibration for each cylinder individually.

An issue for marketability of the HCCI engine is high values of d_p, causing audible noise. The problem is discussed in [Andreae *et al.*, 2007], and it is concluded that noise is mainly related to dp/dt, pressure derivative with respect to time. The acceptable limit for dp/dt is said to vary with engine design, but levels in the range of 3–9.6 MPa/ms

have been reported in the literature. In the work presented here, d_p is reported in terms of pressure derivative with respect to crank angle. At the engine speed used in the fumigation experiments, 1450 rpm, a limit of audible noise at 5 MPa/ms corresponds to 5.75 bar/CAD. By constantly monitoring d_p using the closed-loop controller it was possible to keep d_p in the allowable range, contrary to most previous high-load HCCI studies.

The controllers were designed to enable steady-state experiments. Open-loop experiments showed that the process could likely be operated in open-loop, but that d_p is very sensible to operating parameters such as load. It is therefore possible that adequate transient performance would require closed-loop control. The controller used here, which was slow and did not consider couplings between the two inputs and the two outputs would then not be adequate, instead a model-based controller taking into account the process dynamics is required. There are several factors to consider in developing such a controller. A faster controller will be less robust, wherefore nonlinear dynamics with respect to operating point must be considered. Also, the non-Gaussian character of the process noise will require special attention in a faster control design.

Control of direct injection diesel operation

Purpose In low-temperature combustion diesel engines, there are clear trade-offs between NO_x and soot emissions, brake efficiency, and audible noise. To comply with emissions standards, the range where all variables are acceptable becomes very narrow. Closed-loop control based on feedback from pressure sensors is a more robust way of determining operating conditions resulting in low emissions than open-loop control that relates emissions to actuator settings alone.

Benefits of control Empirical maps were used to relate an emissions cost functions to measured variables α_{50} and α_{ID}, and system identification was used to find models from u_{SOI} and u_{EGR} to the measured variables. LQG control design was then successfully used to minimize the cost function during transients. Because the level curves of the cost function are heavily skewed, where deviations in some directions are much more severe than others, an optimization-based control

method such as LQG makes the design procedure much easier for this MIMO process than a control design method based on e.g., pole placement.

To make the control design approach more widely applicable, it is necessary to consider more inputs either as control variables or measured disturbances, such as speed, load, injection pressure and boost pressure. It is also necessary to consider actuator constraints. This could be done either by using MPC rather than LQG, or by adjusting some other variable to keep the control variables within their operating range, c.f. the mid-ranging results in Chapter 4.

The control design could be integrated into a complete engine control system as a low-level control loop that maintains measured process variables at desired setpoints and optimize the transient trajectories when disturbances take the process away from its setpoints. A higher-level control loop should then be included for setpoint optimization, either determining optimal setpoints according to a static pre-determined map as was done here, or by closed-loop extremum-seeking control.

Summary

Three different engine set-ups designed for low-emissions combustion were studied, where benefits of closed-loop control were verifed in all experiments. The control objective varied throughout the experiments; in the first case it was disturbance rejection and stabilization, in the second case automatic calibration to facilitate laboratory experiments, and in the third case emissions optimization during transients.

In all three set-ups, it could be seen that there are large differences in terms of the actuator settings required to maintain the same combustion characteristics in all cylinders. All three solutions for control design could successfully harmonize combustion between the cylinders. When using actuators that are common to all cylinders, the control design methodology was modified to explicitly handle this limitation.

7.2 Future work

Future work is planned to build on the results from the direct injection engine configuration. To extend the LQG control approach to work

over an entire driving cycle, it is necessary to consider the nonlinear dynamics of the process. Some gain-scheduled or multi-model approach is then necessary. Both the emissions mapping and the system identification of dynamical models must then be extended to handle the entire speed-load plane. It is an open question whether it is best to obtain such models from empirical data, physical modeling, or a combination of both.

Actuator constraints are inherent in all control systems, and could likely better be taken into account using MPC rather than LQG control design.

More work is required concerning the choice of feedback variables. If cylinder pressure sensors are used, a large number of feedback variables could be extracted in each cycle. In this work, α_{50}, α_{ID}, IMEP_n, and d_p were used, depending on the application. Feedback variables that can be easily computed and that can predict emissions in a robust way are desired. It is also of interest to examine the quality of the information that could be extracted from alternative sensors such as knock sensors.

8

Bibliography

Agrell, F., H. Ångström, B. Eriksson, J. Wikander, and J. Linderyd (2003): "Transient control of HCCI through combined intake and exhaust valve actuation." In *SAE Technical Paper 2003-01-3172*.

Agrell, F. and J. Linderyd (2005): "Swedish patent: SE525677 C, Arrangemang och förfarande för att styra en förbränningsmotor."

Akihama, K., Y. Takatori, K. Inagaki, S. Sasaki, and A. M. Dean (2001): "Mechanism of the smokeless rich diesel combustion by reducing temperature." In *SAE Technical Paper 2001-01-0655*.

Alger, T., S. Hanhe, C. E. Roberts, and T. W. Ryan (2005): "The heavy duty gasoline engine - a mutli-cylinder study of a high efficiency, low emission technology." In *SAE Technical Paper 2005-01-1135*.

Allison, B. and A. Isaksson (1998): "Design and performance of mid-ranging controllers." *Journal of Process Control*, **8(5,6)**, pp. 469–474.

Andreae, M. M., W. K. Cheng, T. Kenney, and J. Yang (2007): "On HCCI engine knock." In *SAE Technical Paper 2007-01-1858*.

Aoyama, T., Y. Hattori, J. Mizuta, and Y. Sato (1996): "An experimental study on premixed-charge compression ignition gasoline engine." In *SAE Technical Paper 960081*.

Åström, K. J. and B. Wittenmark (1997): *Computer-Controlled Systems, 3rd edition*. Prentice Hall, Upper Saddle River, New Jersey.

Bengtsson, J. (2004): *Closed-Loop Control of HCCI Engine Dynamics*. PhD thesis, ISRN LUTFD2/TFRT–1070-SE, Department of Automatic Control, Lund University.

Canova, M., F. Chiara, M. Flory, S. Midlam-Mohler, Y. Guezennec, and G. Rizzoni (2007): "Dynamics and control of DI and HCCI combustion in a multi-cylinder diesel engine." In *Proc. for the Fifth IFAC Symposium on Advances in Automotive Control*, pp. 479–486. Aptos, CA.

Dec, J. E. (1997): "A conceptual model of DI diesel combustion based on laser-sheet imaging." In *SAE Technical Paper 970873*.

DieselNet (2007): "Emissions standards, United States, heavy-duty diesel truck and bus engines." www.dieselnet.com/standards/us/hd.php, Revision 2007.09a, Jan 17 2008.

DieselNet (2008): "Emissions standards, European Union, heavy-duty diesel truck and bus engines." www.dieselnet.com/standards/eu/hd.php, Revision 2008.01, Jan 17 2008.

Environmental Protection Agency (2001): "Control of air pollution from new motor vehicles: Heavy-duty engine and vehicle standards and highway diesel fuel sulfur control requirements; final rule."

Guzzella, L. and A. Amstutz (1998): "Control of diesel engines." *IEEE Control Systems Magazine*, **18(5)**, pp. 53–71.

Haddad, W. M. and R. Moser (1994): "Optimal dynamic output feedback for nonzero set point regulation: The discrete-time case." *IEEE Transactions on Automatic Control*, **39(9)**, pp. 1921–1925.

Hafner, M., M. Schüler, O. Nelles, and R. Isermann (2000): "Fast neural networks for diesel engine control design." *Control Engineering Practice*, **8(11)**, pp. 1211–1221.

Haraldsson, G., J. Hyvonen, P. Tunestål, and B. Johansson (2002): "HCCI combustion phasing in a multi-cylinder engine using variable compression ratio." In *SAE Technical Paper 2002-01-2858*.

Heywood, J. B. (1988): *Internal Combustion Engine Fundamentals*. McGraw-Hill, New York.

Iwabuchi, Y., K. Kawai, T. Shoji, and Y. Takeda (1999): "Trial of new concept diesel combustion system - premixed compression-ignited combustion." In *SAE Technical Paper 1999-01-0185*.

Johansson, R. (1993): *System Modeling and Identification*. Prentice Hall, Englewood Cliffs, New Jersey.

Karlsson, M., K. Ekholm, P. Strandh, R. Johansson, P. Tunestål, and B. Johansson (2007): "Closed-loop control of combustion phasing in an HCCI engine using VVA and variable EGR." In *Proc. for the Fifth IFAC Symposium on Advances in Automotive Control*, pp. 517–524. Monterey, CA.

Kim, D., M. Y. Kim, and C. S. Lee (2004): "Effect of premixed gasoline fuel on the combustion characteristics of compression ignition engine." *Energy & Fuels*, **18**, pp. 1213–1219.

Kimura, S., O. Aoki, H. Ogawa, and S. Muranaka (1999): "New combustion concept for ultra-clean and high-efficiency small DI diesel engines." In *SAE Technical Paper 1999-01-3681*.

Lewander, M., K. Ekholm, B. Johansson, P. Tunestål, N. Milovanovic, N. Keeler, and T. Harcombe (2008): "Investigation of the combustion characteristics with focus on partially premixed combustion in a heavy duty engine." In *Submitted to the 2008 SAE International Powertrains, Fuels and Lubricants Congress*.

Martinez-Frias, J., S. Aceves, D. Flowers, J. Smith, and R. Dibble (2000): "HCCI control by thermal management." In *SAE Technical Paper 2000-01-2869*.

Musculus, M. P. B. (2006): "Multiple simultaneous optical diagnostic imaging of early-injection low-temperature combustion in a heavy-duty diesel engine." In *SAE Technical Paper 2006-01-0079*.

Najt, P. M. and D. E. Foster (1983): "Compression-ignited homogeneous charge combustion." In *SAE Technical Paper 830264*.

Noehre, C., M. Andersson, B. Johansson, and A. Hultqvist (2006): "Characterization of partially premixed combustion." In *SAE Technical Paper 2006-01-3412*.

Noguchi, M., Y. Tanaka, T. Tanaka, and Y. Takeuchi (1979): "A study on gasoline engine combustion by observation of intermediate reactive products during combustion." In *SAE Technical Paper 790840*.

Odaka, M., H. Suzuki, N. Koike, and H. Ishii (1999): "Search for optimizing control method of homogeneous charge diesel combustion." In *SAE Technical Paper 1999-01-0184*.

Olsson, J., P. Tunestål, and B. Johansson (2001): "Closed-loop control of an HCCI engine." In *SAE Technical Paper 2001-01-1031*.

Olsson, J., P. Tunestål, B. Johansson, S. Fiveland, R. Agama, M. Willi, and D. Assanis (2002): "Compression ratio influence on maximum load of a natural gas fueled HCCI engine." In *SAE Technical Paper 2002-01-0111*.

Onishi, S., S. H. Jo, K. Shoda, P. D. Jo, and S. Kato (1979): "Active thermo-atmosphere combustion (ATAC)—a new combustion process for internal combustion engines." In *SAE Technical Paper 790501*.

Ortner, P. and L. d. Re (2007): "Predictive control of a diesel engine air path." *IEEE Transactions on Control Systems Technology*, **15(3)**, pp. 449–456.

Ryan, T. and T. J. Callahan (1996): "Homogeneous charge compression ignition of diesel fuel." In *SAE Technical Paper 961160*.

Scania (2006): "Scania to launch Euro 5 engine with EGR in 2007, press release, www.scania.com/news/press_releases/2006/q4/n06051en.asp."

Shaver, G. M., M. Roelle, and J. C. Gerdes (2006): "A two-input two-output control model of HCCI engines." In *Proc. American Control Conference*, pp. 472–477. Minneapolis, MN.

Solyom, S. and S. Eriksson (2006): "Mid-ranging scheme for idle speed control of SI engines." In *SAE Technical Paper 2006-01-0608*.

Strandh, P. (2006): *HCCI Operation—Closed Loop Combustion Control Using VVA or Dual Fuel*. PhD thesis, ISRN LUTMDN/TMHP–06/1039-SE, Department of Energy Sciences, Lund University.

Strandh, P., J. Bengtsson, R. Johansson, P. Tunestål, and B. Johansson (2004): "Cycle-to-cycle control of a dual-fuel HCCI engine." In *SAE Technical Paper 2004-01-0941*.

Strandh, P., J. Bengtsson, R. Johansson, P. Tunestål, and B. Johansson (2005): "Variable valve actuation for timing control of a homogeneous charge compression ignition engine." In *SAE Technical Paper 2005-01-0147*.

Takeda, Y., N. Keiichi, and N. Keiichi (1996): "Emission characteristics of premixed lean diesel combustion with extremely early staged fuel injection." In *SAE Technical Paper 961163*.

Thring, R. H. (1989): "Homogeneous-charge compression-ignition (HCCI) engines." In *SAE Technical Paper 892068*.

Turns, S. R. (2000): *An Introduction to Combustion - Concepts and Applications, 2nd Edition*. McGraw-Hill Internation Editions, Singapore.

Volvo Group (2004): "Volvo Trucks: SCR infrastructure starts to take shape, press release, www.volvo.com/trucks/global/en-gb/newsmedia/pressreleases."

Volvo Group (2007): "Volvo displays carbon-dioxide-free trucks, press release, www.volvo.com/group/global/en-gb/newsmedia/pressreleases/2007/."

Yilmaz, H. and A. Stefanopoulou (2003): "Control of charge dilution in turbocharged diesel engines via exhaust valve timing." In *Proc. American Control Conference*, pp. 761–766.

Zaidi, K., G. E. Andrews, and J. H. Greenhough (1998): "Diesel fumigation partial premixing for reducing ignition delay and amplitude of pressure fluctuations." In *SAE Technical Paper 980535*.

Zhao, F. and T. Asmus (2003): "HCCI control and operating range extension." In Zhao *et al.*, Eds., *Homogeneous Charge Compression Ignition (HCCI) Engines—Key Research and Development Issues*. SAE.

Nomenclature

Symbols

α_{10}	Crank angle degree of 10 % heat released
α_{50}	Crank angle degree of 50 % heat released
α_{ID}	Ignition delay, $\alpha_{ID} = \alpha_{10} - u_{SOI}$
η_b	Brake efficiency
λ	Equivalent air/fuel-ratio
θ	Crank angle degree
d_p	Maximum pressure derivative over an engine cycle
dQ	Heat release rate
N	Engine speed
p	Cylinder pressure
p_{in}	Intake pressure
Q	Cumulative heat released during cycle
r_{EGR}	EGR rate
T	Temperature
u_{EGR}	Position of EBP valve
u_{IVC}	Crank angle degree of inlet valve closing
u_{SOI}	Crank angle degree of start of injection
V	Volume
V_D	Displaced volume
W_{in}	Injected fuel energy per cycle and cylinder

Acronyms

ATDC	After top dead center
BMEP	Brake mean effective pressure
BTDC	Before top dead center

CAD	Crank angle degree
CAN	Controller area network
CI	Compression ignition
CO	Carbon monoxide
CO_2	Carbon dioxide
EBP	Exhaust back pressure
EGR	Exhaust gas recirculation
EVC	Exhaust valve closing
EVO	Exhaust valve opening
FIFO	First in first out
HC	Hydrocarbons
HCCI	Homogeneous charge compression ignition
$IMEP_n$	Net indicated mean effective pressure
IVC	Inlet valve closing
IVO	Inlet valve opening
LQG	Linear quadratic gaussian (controller)
MIMO	Multiple input multiple output
MK	Modulated kinetics
MPC	Model predictive control
NO	Nitric oxide
NO_2	Nitrogen dioxide
NO_x	Oxides of nitrogen
PCI	Premixed compression ignited
PFI	Port fuel injection
PI	Proportional integral (controller)
PIC	Peripheral interface controller
PID	Proportional integral derivative (controller)
PM	Particulate matter
PPC	Partially premixed combustion
PREDIC	Premixed lean diesel combustion

SCR	Selective catalytic reduction
SI	Spark ignition
SOI	Start of injection
TDC	Top dead center
VAF	Variance accounted for
VCR	Variable compression ratio
VGT	Variable geometry turbo
VVA	Variable valve actuation

Department of Automatic Control
Lund University
Box 118
SE-221 00 Lund Sweden

Document name
LICENTIATE THESIS

Date of issue
March 2008

Document Number
ISRN LUTFD2/TFRT--3243--SE

Author(s)
Maria Karlsson

Supervisor
Rolf Johansson
Per Tunestål
Per Hagander

Sponsoring organisation
Vinnova, Volvo Powertrain

Title and subtitle
Control Structures for Low-Emission Combustion in Multi-Cylinder Engines

Abstract

Traditionally, heavy-duty diesel engines have high efficiencies but also high emissions of NO_x and soot particles. New engine concepts show the potential to retain diesel-like efficiencies while reducing emissions by forming a completely or partially homogeneous mixture of fuel and air prior to ignition through compression. The long ignition delay required to form this homogeneous mixture makes the combustion process less predictable and inherently more difficult to control.

This thesis summarizes work on control structures for three different setups of such low-emissions combustion engines. In a port-fuel injection engine, it was shown that combining two control variables in a mid-ranging control structure can address the problem of actuator saturation. In a fumigation engine, control was proven to be a powerful tool for automatic calibration in a laboratory setting. In a direct-injection engine, LQG controllers were designed to optimize an emissions trade-off cost function during transients. Experiments were performed on a six-cylinder heavy-duty engine, and multi-cylinder effects and complications were explicitly considered in the work.

Key words
engine control, HCCI engine, fumigation, mid-ranging control, LQG control

Classification system and/or index terms (if any)

Supplementary bibliographical information

ISSN and key title
0280–5316

ISBN

Language
English

Number of pages
96

Recipient's notes

Security classification